INVESTIGATION OF BENCH METHODS FOR DETERMINING STIFFNESS OF SOLID ANKLE-FOOT ORTHOSES

By

Komaris Dimitrios Sokratis (Dipl.-Ing.)

Department of Biomedical Engineering

University of Strathclyde

August 2014

This thesis is submitted to the University of Strathclyde in partial fulfillment of the requirements for the degree of Master of Science in Biomedical Engineering.

Declaration of Authenticity and Author's Rights

This thesis is the result of the author's original research. It has been composed by the author and has not been previously submitted for examination which has lead to the award of a degree.

Signed:

Date:

Acknowledgments

To begin with, I wish to express my gratitude to my supervisor Mr. Stephan Solomonidis for all his support during this year. His advice and assistance were the driving force and the catalyst for the completion of my master thesis. Thanks for always being there for me, keen to discuss the progression of my project.

My greatest gratitude goes also to Mr. John Maclean for his guidance with the Instron E10000 and to Mr. Stephen Murray for helping me build a terrific dummy leg for my tests.

Thanks to my friends, Andre Attard, Nadira Salah and Georgia Tarfali for helping me with my studying and the testing of the ankle-foot orthosis.

Finally, many thanks to my Katerina, my friends and my family, and especially Nikos, for all the support they gave me over this year.

Socratis

Abstract

The applications of ankle-foot orthoses (AFOs) are nowadays the most common treatment for the compensation of neuromuscular disorders usually caused by stroke and spinal cord or peripheral nerve injuries. The biomechanical functions of plastic AFOs are determined by their thickness, the material selection and their geometry. The geometry, also known as trim-line, reflects the stiffness in relationship to the range of motion that the AFO allows at the talocrural joint (Lin and Bono, 2010). Their design, however, is mainly empirical due to a lack of evidence-based research on their geometrical characteristics (Papi, 2012). Therefore, experimental data are critical for the optimization of AFOs' characteristics.

This project aims to investigate the different experimental methods currently utilized for determining the stiffness of homo-polymer and co-polymer polypropylene AFOs with different trim lines. The strengths and weaknesses of each experimental method were analysed and the most reliable techniques has been implemented in order to determine the relationship of AFOs' mechanical properties and their geometry. Three AFOs were tested in total: a 4.6 mm black co-polymer solid AFO, a 6mm homo-polymer solid AFO and a 4.6 co-polymer solid AFO with carbon fibre shape corrugations. The experimental procedure had two objectives:

1. To fabricate and document an effigy leg suitable for the stiffness testing of an AFO.

2. To measure and compare the stiffness of an AFO with/without the presence of the effigy leg by means of different stiffness-measuring methods.

The results of this study indicate that the difference in stiffness when a leg is introduced in an AFO is noteworthy while the difference in the results between different methods is considerable as well. It is believed that the cause of this

variation is that the manual methods are sensitive to creep and thus the AFO seems to be more flexible when measured manually.

The outcome of this study would be beneficial for biomedical engineers and practitioners involved with the manufacturing of custom fabricated AFOs.

Table of Contents

List of figures

List of tables

List of acronyms

Abbreviation:	Definition:
AAFO	An Articulated ankle-foot orthosis is an orthosis with a joint around the ankle allowing a more natural movement in the sagittal plane while limiting the range of motion in other planes.
AFO	According to ISO 8549, an orthosis, and thus also an ankle-foot orthosis, is “an externally applied device used to modify the structural and functional characteristics of the neuromuscular and skeletal systems.”
F.E.A.	According to Autodesk, a software developing company, finite element method works by breaking down a real object into a large number of elements, such as little cubes. Mathematical equations help predict the behaviour of each element. A computer then adds up all the individual behaviours to predict the performance of the actual object.
F.E.M.	Finite element model
GRAFO	Ground Reaction Ankle-foot orthosis

1 Introduction

1.1 Ankle-foot orthosis (AFO)

According to the oxford dictionary, an orthosis (plural: orthoses), originates from the Greek *orthōsis* (ορθώσης) 'making straight', from *orthoun* 'set straight' and refers to a brace used for the "correction of disorders of the limbs or spine to correct alignment or provide support". An Ankle-foot orthosis (AFO) is a device worn on the lower part of the leg to provide direct control of the motion and alignment of the ankle and foot. According to the International Standards Organization, the AFO is defined as "an orthopedic device which encompasses the ankle joint and the whole or part of the foot and is externally applied in order to modify the structural and functional characteristics of the neuromuscular and skeletal systems". AFOs are prescribed to patients with neuromuscular disorders which are usually caused by stroke or spine and peripheral nerve injuries in order to correct gait abnormalities associated to (Bregman et al., 2009):

1. Inadequate ankle dorsiflexion[1] during the swing phase.

2. Reduced stability in stance phase.

3. Abnormal heel strike.

According to the American Board for Certification in Orthotics, Prosthetics and Pedorthics (2007), AFOs are the most frequently used orthoses, making up about 26% of all orthoses prescribed by certified orthotists in the United States and twice as many than any other type of orthosis. An ankle-foot orthosis is commonly made of polypropylene with a geometry that resembles an "L", with the proximal part positioned posterior of the calf and the distal segment located under the foot. Typically, they are attached to the limb with a Velcro strap; their thickness generally allows the patient to wear shoes over the orthosis. Throughout the last few decades

[1] The reader may refer to Appendix 1: The planes of motion of the human foot and the anatomical terms of motion.

several other materials such as subortholen, acrylics, composite carbon fibres, cork and polyethylene foams were used during the fabrication procedure of ankle-foot orthoses. Polypropylene-based plastics are the most common material choice due to their lightweight and high stiffness which allows the orthotist to counter the forces responsible for gait abnormalities (e.g. drop foot).

Figure 1 Ankle-foot orthoses (Korthotics.com.au, 2014).

Based on the fabrications procedure, ankle-foot orthoses can be divided in two categories:

1. Prefabricated AFOs in different sizes and geometries to fit the needs of the end user.
2. Custom made AFOs from a positive mould obtained from the patient and/or with Computer-aided design (CAD) systems.

Figure 2 Fabrication procedure of a custom made polypropylene AFO (The International Committee of the Red Cross (ICRC), 2006).

Patient evaluation, casting and fabrication of the orthosis are carried out in agreement with prosthetic and orthotic (P&O) standards. The International Committee of the Red Cross published in 2006 (The International Committee of the Red Cross (ICRC), 2006) a manufacturing guideline in order to describe methods for fabricating ankle-foot orthoses made out of polypropylene. In this guideline, the ankle-foot orthoses are classified in four categories based on their design:

1. *Flexible* AFOs or *Posterior Leaf Spring* AFOs. This AFO is only prescribed in patients with limited dorsiflexion weakness (drop foot). It is not suitable when the patient is suffering from an increased degree of spasticity/tone or there is a need of knee control. In many cases, this type is not suitable for stroke patients.

2. *Rigid* or *Solid* AFOs. A Rigid AFO blocks all movement at the ankle joint. They are usually prescribed for stroke patients suffering from high tone or spasticity in their plantarflexors.

3. AFO *with Tamarack Flexure Joint*, *Hinged* or *Articulated* AFO. Typically, hinged AFOs can block plantarflexion but allows the ankle to dorsiflex freely. This AFO is often prescribed to patients with subtalar joint or mediolateral unsteadiness.

4. AFO *Anti-talus* or *Ground Reaction* orthosis (GRAFO). This design of AFO is practically a solid AFO which is designed to maximize the control of the knee flexion during stance phase.

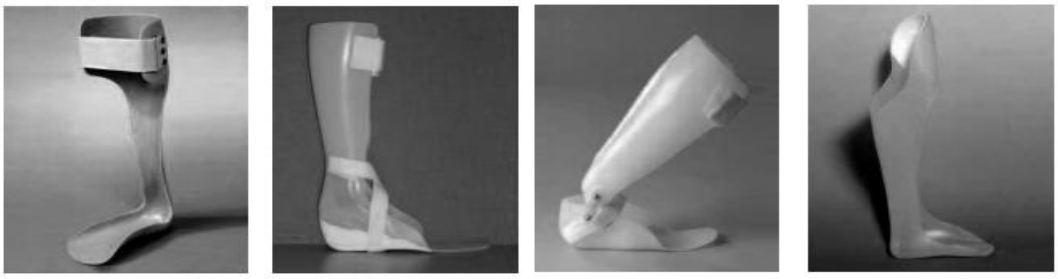

Figure 3 Different types of AFO; from left to right: Posterior Leaf, Solid, Hinged and GR AFO AFO (The International Committee of the Red Cross (ICRC), 2006).

An AFO is generally subscribed to patients with gait disorders that affect the muscle function such as stroke, spinal cord injury, polio, multiple sclerosis or severe flat foot. Nowadays, the vast majority of the patients using an AFO have suffered a stroke and they are left with a foot deformity (figure 4). According to the British Heart Foundation (Petersen, Mockford and Rayner, 1999), stroke is the fourth largest cause of death: there are more than 150,000 strokes in the United Kingdom per year. In addition, more than half a million stroke survivors are suffering from different types of paralysis such as hemiplegia, a condition responsible for asymmetric gait, slow speed of waking and difficulties with balance. In stroke rehabilitation, prefabricated AFOs are rarely used; since they cannot be personalized, the fitting is inadequate and they are not preferred for chronic usage. Furthermore, among the four different types of AFO described above, the solid design is typically used in post-stroke patients. As a result, custom-made, solid AFOs are used and discussed in this study.

Figure 4 Common foot deformities (Ufrgs.br, 2014).

1.2 Aims of the thesis

The effects of the ankle-foot orthosis on gait stability and walking balance are well documented. Romkes and Brunner (2002) have studied the effect of different designs of AFOs in twelve hemiplegic cerebral palsy patients walking with and without their orthosis. In this study the benefits of a hinged AFO in controlling the patients' plantarflexion are reported. Rose et al. (2009) reported the improvements in gait quality in thirty five children affected by cerebral palsy measured by the gait deviation index. Neviani et al. (2012) quantified the satisfaction of eleven cerebral palsy patients using the QUEST questionnaire (Quality of life in Essential Tremor Questionnaire) and reported that the patients were highly satisfied even with a minor improvement in their gait. A 3-D gait analysis was used by Ploeger et al. (2014) to evaluate the prescription of ankle-foot orthosis to sixteen polio survivors. In this study, patients wearing an AFO had improved walking speed and stability compared to a walking trial with only their shoes. The effects of AFOs on gait stability, speed and balance during walking are documented in several reports (Xu et al, 2014; Tyson, 2013; Chen et al., 2010).

Nevertheless, only a few studies (Yamamoto et al., 1993; Bregman et al., 2010; Papi, 2012) reported on the effects and contribution of the AFO's stiffness on patients' ambulation. The results from these reports are infrequently applied in clinical practice. This project aims to investigate the different experimental methods utilized nowadays for determining the stiffness of polypropylene AFOs with different trim lines (geometry). The strengths and weaknesses of each experimental method will be analysed and the most reliable technique will be implemented in order to determine the relationship of AFO's mechanical properties and their geometry. The outcome of this study would be beneficial for biomedical engineers and practitioners involved with the manufacturing of custom fabricated AFOs. This study will have a positive effect in clinical practice, knowing that nowadays, most orthotists still prescribe and design an orthosis based on their empirical techniques and not on scientific data.

1.3 Layout of thesis

The work conducted to fulfill the Master's aims is outlined in this project and is divided in chapters as follows:

Chapter 1 describes the different types of AFOs and the way they affect the patient's gait. This chapter concludes with the importance of the trimline in the mechanical properties of the orthosis.

Chapter 2 presents an overview of the different methods for determining the stiffness of an ankle-foot orthosis. The strengths and weaknesses of each experimental bench method are analysed and criticized.

Chapter 3 focuses on the testing procedure used in this study. The stiffness of four different types of AFO was tested in an Instron ElectroPuls™ E10000.

Chapter 4 outlines the results obtained by the testing described earlier in Chapter 3.

The findings are analysed in Chapter 5 and finally, Chapter 6 critically discusses the methods that were described earlier in Chapter 2 and the results obtained by the testing in Instron E10000. Chapter 6 concludes with recommendations for future studies.

2 Literature review

2.1 Introduction

The applications of ankle-foot orthoses (AFOs) are nowadays the most common treatment for the compensation of neuromuscular disorders usually caused by stroke and spinal cord injuries. The mechanical function of the orthosis must match the needs of the patient (Kobayashi et al., 2011). Clinical assessments (Sumiya et al.,1996) verified that there is an optimum match between the stiffness of the ankle-foot orthosis and the walking deformities of each patient. Thus, the methods used to determines the stiffness of an AFO must be critiqued in order for this decision making procedure to be optimal.

2.2 Stiffness of the AFO

The biomechanical function of plastic AFOs is determined by their thickness, the material selection and their geometry. Typically, the material of choice for an AFO is a polypropylene-based plastic due to its lightweight and stiffness. The thickness is usually less that 1cm since the orthosis must allow the patient to wear also shoes and walk comfortably. The geometry, also known as trim-line, reflects the stiffness in relation to the range of motion that the AFO allows at the talocrural joint (Lin and Bono, 2010). Their design, however, is mainly empirical due to a lack of evidence-based research on their geometrical characteristics (Papi, 2012). Therefore, experimental data are critical for the optimization of AFO's characteristics.

Nowadays, different AFO trimlines are subscribed for different gait abnormalities. Figure 5 shows a *solid* AFO and three *Posterior Leaf Spring* AFOs with different trimlines. AFO stiffness can be measured either computationally or mechanically. Mechanical testing can be done with either (1) bench or (2) functional methods; (3) computational methods typically refer to finite element analysis. In the bench methods, the AFO is attached to a custom made device designed for the

stiffness measurement. In functional approach, the measurement is held while a patient walking with an AFO. Those three approaches are discussed in the following chapters.

Figure 5 Ankle-foot orthoses trim-lines: a solid AFO and three Posterior Leaf Spring AFOs (Rehabmart.com, 2014)

2.2.1 Mechanical analysis

2.2.1.1 Bench testing analysis

Different devices were designed and a variety of transducers were used for the stiffness testing of the AFOs. A literature review was conducted in Google Scholar, Scopus and Elsevier; the key-words used were: AFO, ankle-foot orthosis, stiffness and rigidity. In the literature, eight articles describing methods for determining the stiffness of an AFO were found. Those methods are critically described in Chapter 2.3 entitled “Bench testing methods for determining stiffness of ankle-foot orthosis”.

According to the author's viewpoint, the following parameters were considered during the investigation and the evaluation of those eight bench testing methods:

1. Is the testing method accurate and repeatable? This can be established by statistical analysis of the results such as the standard deviation of the measurements, G-study (Based on the Generalizability theory, a G-study is

used to determine the reproducibility of the measurement) or coefficient of repeatability (Kobayashi et al., 2011). According to Kobayashi et al. the G-study can determine the influence of different sources of error in measurements by identifying the minimum detectable variation while repeatability coefficient can quantify the repeatability of the measurement protocol.

2. Does the report include comprehensible and clear data regarding the methodology followed in order to assist the recurrence of the experiment and confirmation of the results?

3. How is AFO stiffness defined? The stiffness of the orthosis should be calculated as the moment applied to the ankle joint per angle of deformation (Nm/Degree). Some studies define stiffness differently; for instance Lunsford et al. (1994) defines the AFO's stiffness as the force needed to cause 10° of dorsiflexion.

4. Is the testing static or is the stiffness of the AFO recorded in a range of motion? A Continuous testing procedure can generate more precise stiffness graphs. Nevertheless, the choice of the transducer is essential: e.g. dial gauges can only measure statically.

5. Is the device applicable in clinical testing? Is the device applicable in industrial testing or can it be used for quality control? Parameters such as cost-efficiency, ease to build, portability of the apparatus and convenience of the method should be considered.

6. Is the test destructive for the AFO? E.g. is the AFO secured in the device with G-clamps or with bolts? Typically, an AFO with holes in the sole cannot be used in patients after the testing.

7. Can the test mimic the loading pattern during normal gait? This is probably the most important parameter in bench testing. It is a common approach to introduce an effigy leg with an ankle joint or even with a metatarsal joint in

order to indirectly load the AFO through the dummy leg. It is also important to place the ankle joint of the effigy leg as close as possible to the center of the axis passing through the AFO's malleolli protuberances. Also we have to consider that the loading of the AFO is related to the pathology of the patient. The material of the surrogate leg should be as close as possible to that of a human leg and it should imitate the viscoelastic properties of the skin. Ideally, shoes should be included in the testing procedure. It should be noted that the absence of the effigy leg also causes abnormal buckling of the AFO in the malleoli region. Finally the range of motion and the angular velocity of the testing should reflect those of patient's gait.

8. Can the apparatus measure the stiffness of the AFO in more than one plane? Chowaniec (1983) reported that during the application of inversion/eversion loads, a deformation in the sagittal[2] plane was recorded by strain gauges. Also, Klasson et al. (1998) reported that the application of moments in the sagittal plane results in translations and angulations in all other planes.

9. Can it be used in every kind of AFO? A device used for the measurement of the stiffness of an articulated AFO (hinged AFO) is not usually suitable for a non-articulated AFO testing and vice versa.

10. Are the transducer and the loading easily applicable and accurate? E.g. strain gauges might be challenging to place in an AFO and if they are not placed properly results may be altered; also manual loading of the AFO (Sumiya et al., 1996) might be open to operation bias.

11. Does the method require a model or software to analyse the forces and the moments applied? For example load cells and strain gauges require data processing which can be time consuming, complicated and not applicable for clinical use.

[2] The reader may refer to Appendix 1: The planes of motion of the human foot and the anatomical terms of motion.

12. Is it difficult to place the AFO in the device? Are there any errors due to alignment and fixation that might jeopardize the reproducibility of the experiment?

2.2.1.2 Functional analysis

Functional analysis typically involves a walking trial while the patient is wearing the orthosis. The stresses are usually measured via strain gauges (Chu and Feng, 1998), or with testing devices (Yamamoto et al., 1993a; Yamamoto et al., 1993b).

In the study by Yamamoto et al. (1993a) an experimental AFO consisting of a cuff band, a Klenzek joint, a shoe and a potentiometer was designed. This experimental AFO was used to measure moments generated by the orthosis and both the ankle and knee angles in the sagittal plane; the ankle moment was measured with a custom-made force transducer attached to the sole of the shoe, whereas the potentiometer was used for the ankle joint angle measurement. It was reported that the moment produced by the AFO was of lower value compared to the muscle moment produced by the dorsiflexors. Nevertheless, when the hemiplegic patient was walking with the AFO the net moment of the complex muscles/AFO was sufficient for the correction of the gait.

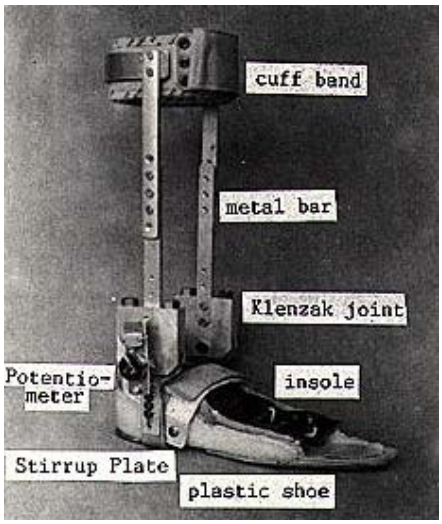

Figure 6 Experimental AFO by Yamamoto et al. (1993a).

In another study by Yamamoto et al. (1993b), a muscle training machine usually found in rehabilitation centers was used. This study is unique since it is describing the only test that used a muscle training apparatus suitable for hemiplegic patients. The patient is asked to place his foot in the machine; during the testing the pulley is rotated automatically with a known constant velocity; the dorsfilexion angles and the moments applied to the human limb are recorded by a computer. The stiffness of four different AFOs was tested and documented in this study: a posterior spring leaf, an anterior spring leaf, a spiral and a side-stay AFO.

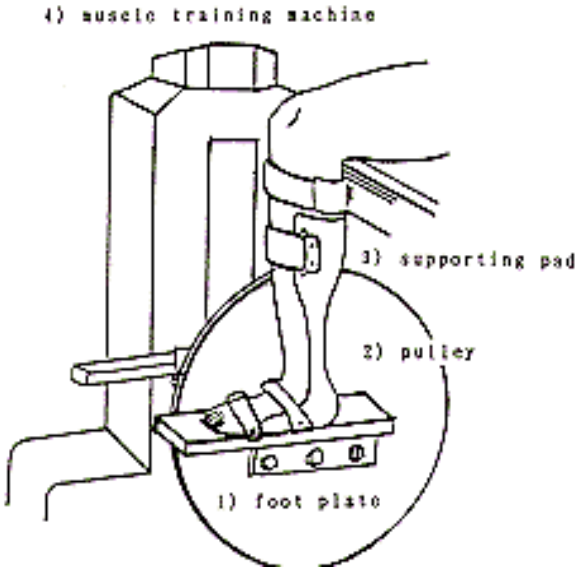

Figure 7 Muscle training machine by Yamamoto et al. (1993b).

Chu and Feng (1998) strain gauged five different polypropylene AFOs. The distribution of the stresses during walking was recorded and the pick stresses showed that the AFO is more likely to fail in the ankle region. Based on this study suggestions about the design of the AFO were made: an orthosis should be made asymmetrically and the calf area must be thicker in order endure the peack of the tensile stresses.

Figure 8 Strain Gauged AFOs by Chu and Feng (1998).

2.2.2 Finite element analysis

Apart from the mechanical testing (functional or bench methods), computational processes (e.g. finite element analysis) were employed in order to simulate and examine the mechanical behavior of the ankle-foot orthosis and the human ankle joint. According to Autodesk, a software developing company, finite element method works by breaking down a real object into a large number of elements, such as little cubes. Mathematical equations help predict the behaviour of each element. The program then adds up all the individual behaviours of the elements to predict the performance of the actual object.

Chu et al. (1995) designed a 3-D finite element model of an AFO and a human leg. The model was composed out of 313 solid elements and the system was considered as linear, elastic and isotropic. The 3-D model was used in order to statically analyse different normal and pathological styles of gait. Subsequently the computational results were validated experimentally (Chu and Feng, 1998). This study revealed that during heel strike maximum compressive stress occurred in the heel area while during toe-off the peak tensile stress was observed in the neck area (ankle area). The model revealed that the stress distribution and magnitude was dependent on the stiffness of the AFO, the elasticity of the soft tissue of the human

limb and the point of heel contact. During the validation of the finite element model (Chu and Feng, 1998), five different types of polypropylene AFO were tested in a walking trial and in a sit-to-stand test. In order to measure the stress, eight strain gauges were attached to each AFO. The stress distribution results were in agreement with the finite element model. Furthermore, parameters such as the mass of the patient, the type of the activity (walking or sit-to-stand) and the trimline of the orthosis are affecting the stresses developed in the AFO.

Uning et al. (2008) used CT scan imaging technology in order to simulate the geometry of the AFO/leg complex. Similar to Chu et al., the model was selected as linear, elastic and isotropic. In this study, the friction between the polypropylene orthosis and the skin was included in the model. No results were published based on this model. Syngellakis et al. (2000) considered large deformation effects and the non linearity of the polypropylene AFO in their finite element model. The mechanical behavior of AFOs with different trimlines was studied and the stiffness of the orthoses for different range of motion was reported.

Finite element analysis provides a reliable and efficient approach for the evaluation of AFOs with different trimlines and geometry or AFOs from different materials. Different simulations can replicate the loading pattern of dissimilar gait abnormalities. With cautious selection of the model's parameters and after the proper validation of the model, finite element analysis can be used for the assessment and the prescription of an AFO or even for the in situ fabrication of an AFO fitted individually to each patient.

2.3 Bench testing methods for determining stiffness of ankle-foot orthosis

2.3.1 Mechanical testing machine (Instron, model 1185) by Major et al. (2004)

Major et al. (2004) investigated the stiffness of four different designs of AFOs: an AFO with forward trim-lines, an AFO with corrugations made over a former

during the casting procedure, an AFO with carbon fibres in the malleoli region and an AFO with forward trim-lines and a Velcro strap. Unfortunately, no other information is given concerning the trimlines of the four different designs and the type of the polypropylene that is was used. All AFOs were prepared from the same polypropylene sheet of 4 mm thickness. In the same study, the authors report that the loading deflection pattern of the AFO is more consistent after the first few loadings. Hence, the first four loading trials were neglected and only the six (6) following trials were used in the analysis. After every cycle, the AFO was removed from the Instron testing machine in order to relax for 15 minutes. A relaxation period after the loading is essential in order to allow the AFOs to recover their mechanical properties: Lunsford et al (1994) reported that the stiffness of a pediatric Rancho AFO is reduced by 30% after a 24-hours loading test. Nevertheless, after 15 minutes of relaxation, the AFO's stiffness was improved by 23% and after 45 minutes the stiffness was almost fully recovered. However, the recovery behavior strongly depends on how much stress is applied to the AFO.

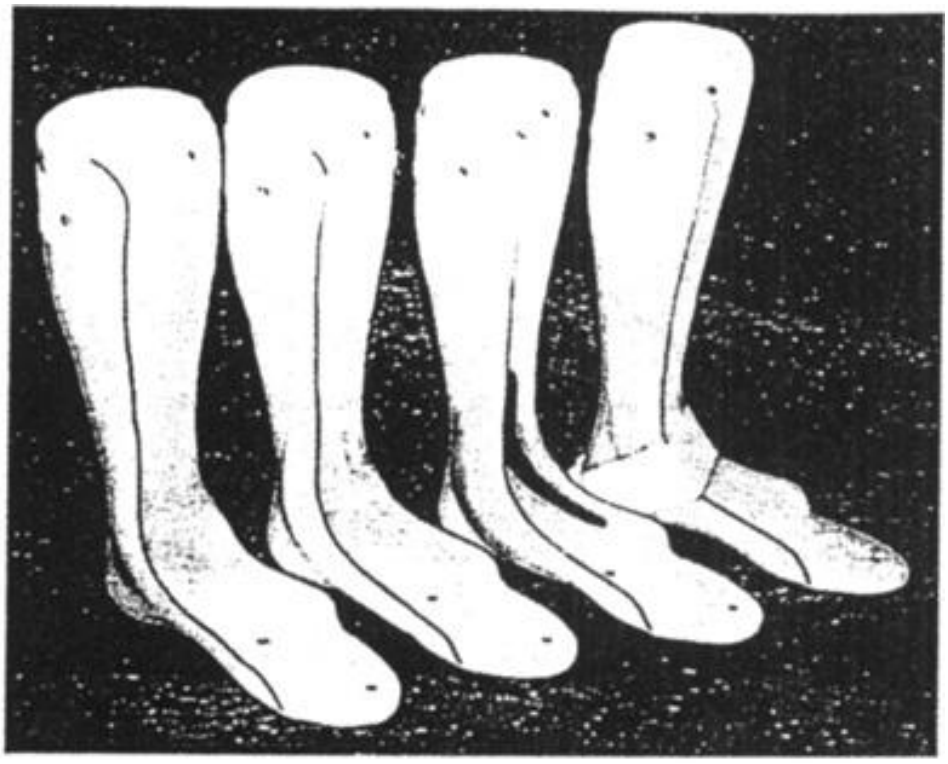

Figure 9 The 4 AFO designs by Major et al. From left to right: AFO with forward trimlines, AFO with corrugations, AFO with carbon fibre inserts, AFO with Velcro strap.

The bench testing was performed on a materials testing machine: an Instron 1185 with a series IX version 5 controller and 1 KN load cell. The mounting of the AFO to the testing machine was achieved by 8mm bolts in similar positions in all cases; nonetheless this procedure is not described in the report. A consistent fixation is essential for the stiffness analysis. If the mounting jigs are not attached at the same position in each AFO then the moment arms will vary between the different AFO designs and thus the measurement method would not be reliable. The sole of the AFO was attached with 3 bolts to a 6mm thick plate made out of steel in order to allow the mounting of the lower moving crosshead.

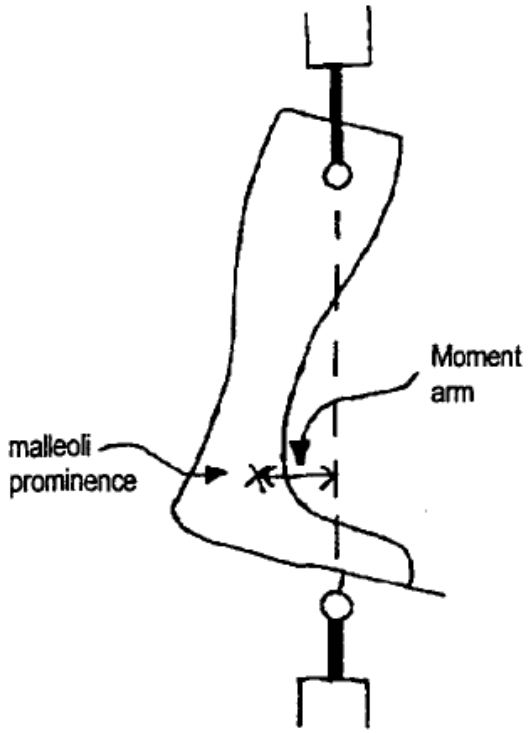

Figure 10 An AFO mounted in the Instron 1185 by Major et al. (2004)

In this test, due to the limitations of the AFO's mounting in the testing machine, the AFOs were tested only in dorsiflexion with a range of motion from 0° to 14° and a compression rate of 2.3°/s. The range used in this test cannot cover the range of motion of the ankle's joint in patients with moving disorders wearing an AFO.

Winter (1990) reported that the motion of the ankle's joint for a normal person is within 7° of dorsiflexion to 20° of plantarflexion. In patients with stroke hemiplegia wearing an ankle-foot orthosis, Fatone et al. (2009) reported that the range of motion is from 10° of dorsiflexion to 5° of plantarflexion. Concerning the loading rate, Yamamoto et al. (1993b) tested four different types of polypropylene AFO in different velocities from 5°/s to 50°/s and reported that the angular velocity does not affect the flexibility of the AFO. Therefore, the difference between the compression rates demonstrated in this test and the loading rates from a patient's gait is considered insignificant. On the other hand, the mounting and the loading of the AFO in this test cannot mimic the loading pattern during ambulation. This is mainly due to the bearing forces from the upper mounting jig during the testing compared to the forces acting from the patient's shank to the AFO during ambulation.

Consequently, the direct mounting of the AFO to the testing machine and the absence of a leg effigy can significantly alter the results obtained. A leg effigy is important in order to substitute the contribution of the patient's leg to the stiffness of the AFO during ambulation. In addition, in these tests, Major et al. reported that the AFO buckled during loading due to the absence of the effigy's internal support. Furthermore, Kobayashi et al. (2011) reported that the viscoelastic properties of the leg's tissue could alter the resistance to deformation and they should be considered during the design of an effigy leg.

In order to measure the stiffness of the AFO the computation of the moment arm is needed. In this study, simple geometrical equations were used in order to calculate the perpendicular distance between the line of action of the force and the axis passing from the ankle. In this report, the ankle axis is assumed as the axis passing from the lateral and medial malleoli prominences of the AFO but as the authors mention, this axis will differ from the actual axis of rotation of the foot/AFO. Thus, using the dimensions in figure 11 and the following equations:

$$D^2 = U^2 + L^2 - 2ULCOS\theta_{(t)}$$

Where $\theta_{(t)}$ is the angle between L and U at time t, and

$$\frac{U}{sinu_{(t)}} = \frac{L}{sinl_{(t)}} = \frac{D_{(t)}}{sin\theta_{(t)}}$$

The moment arm A is equal to:

$$A = \frac{ULsin\theta_{(t)}}{D_{(t)}}$$

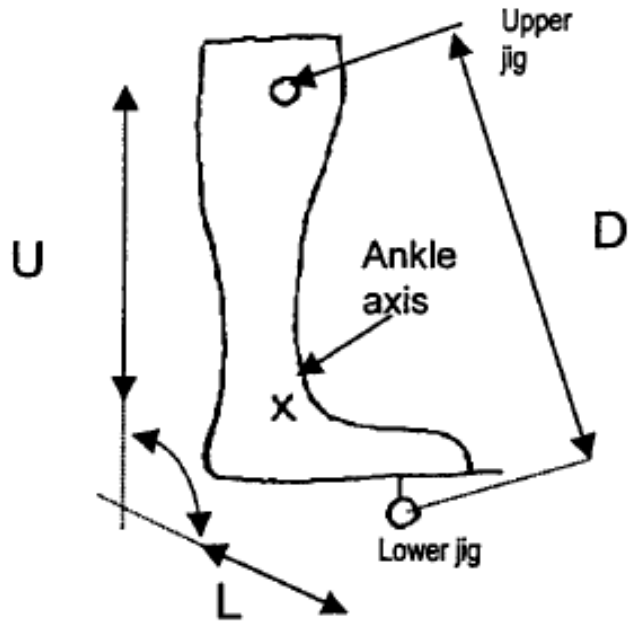

Figure 11 AFO dimensions for the Instron 1185 (Major et el. 2004).

Despite the fact that the distance D was defined as a function of time, the distances U and L were considered as constants, equal to 290mm and 141mm respectively. However, both distances U and L will diminish throughout the test since compression loads will be applied in the sole of the AFO. This assumption can significantly affect the results in a similar test with a greater range of motion (e.g. 7° of dorsiflexion to 20° of plantarflexion). In this experiment, where the range of motion was from 0° to 14° of dorsiflexion the lower moving crosshead moved merely for 2cm and therefore the assumption that the distances U and L are constant can be considered appropriate.

This study demonstrated that the AFO with the forward trimline and the Velcro strap, and the AFO reinforced with carbon fibres demonstrated higher stiffness compared with the other two designs. Moreover the design with the carbon insert started to yield at high loads while the forward trimline design could maintain its stiffness in higher moments. Note that in this study, stiffness is defined as the bending moment applied by the Instron machine per degree of dorsiflexion.

The work of Major et al. aimed to compare the stiffness of four different AFO designs. Similar experiments could be applicable in industry testing or can be used for quality control. Material testing machines such as Instron 1185 can provide results free from operation errors if an appropriate measurement protocol is followed (e.g. control of parameters that influence fixation/alignment and development of a surrogate limb system with a properly aligned ankle joint). On the other hand, the high cost of a material testing machine and the fact that the test is destructive for the orthosis (due to the bolts) renders this test unsuitable for clinical testing. Despite the fact that this testing method cannot mimic the loading and the support of the AFO in ambulation, it can provide accurate and reliable outcomes in a test that aims to compare different designs of orthosis.

2.3.2 Moment measuring device by Sumiya et al. (1996).

Sumiya et al. developed a simple device to measure the stiffness of AFOs made out of low-viscosity materials. The device consists of a leg model, two metal bars, a tensiometer and a protractor. The shank of the effigy leg was composed out of a plaster of Paris cylinder (number 1 in figure 12) and a metallic pipe passing through the cylinder. This plaster cylinder was positioned so as to substitute the calf region. The foot of the effigy leg (number 2) was also made out of moulded plaster of Paris and it was attached to the shank (the metallic pipe) with a hinge at the ankle axis. A plastic AFO is then attached to the effigy leg with screws in the sole of the plaster foot and with a calf cuff.

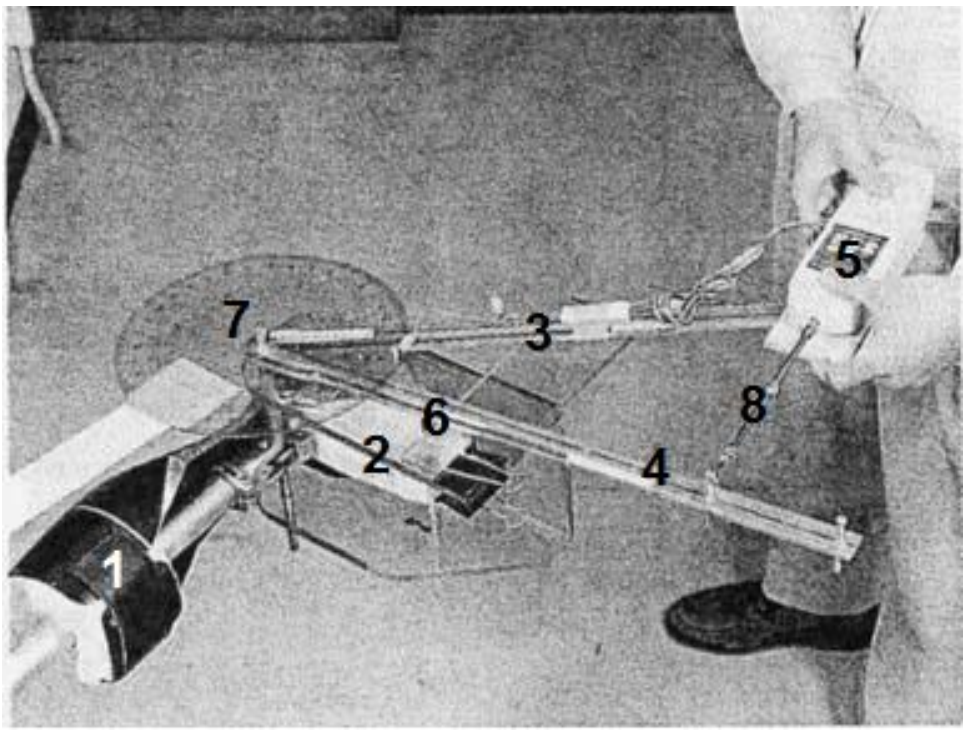

Figure 12 The moment measuring device (modified)[3] by Sumiya et al. (1996)

The edges of the two metal bars (number 3 & 4) were coupled at the ankle joint of the effigy leg in a way to resemble an acute angle. The digital tensiometer (number 5) was then attached to one metallic bar (number 3). The attachment of the tensiometer was made in such a way that the edge of the loadshaft of the tensiometer (number 8) was then attached to the opposite bar (number 4) perpendicularly and at a fixed distance from the ankle axis (0.4 or 0.5 meters). A protractor (number 7) was then placed on top of the metal bars in the ankle joint.

When the tensiometer is pulled, the metallic bar (number 4) is dragging the foot through an upright shaft (number 6) and thus tending to deform the AFO. The force shown in the screen of the tensiometer times the distance from the edge of the loadshaft to the ankle joint is equal to the moment applied to the orthosis. This ankle moment divided by the AFO's angle of deformation (measured with the protractor) represents the stiffness of the AFO. Figure 13 demonstrates the two

[3] Modified by the author of this thesis.

different assemblies used in order to measure the stiffness of the AFO in plantarflexion and in dorsiflexion.

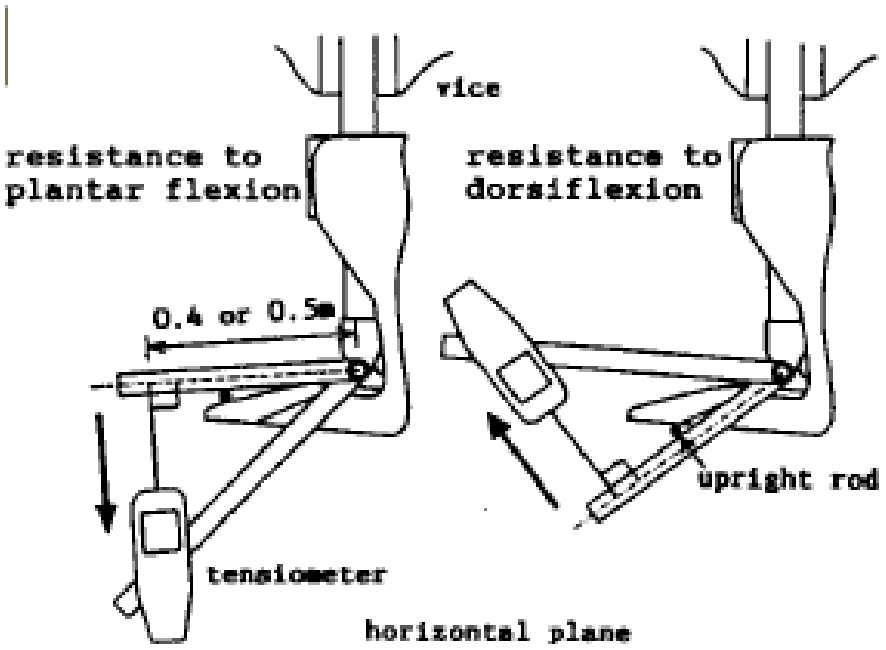

Figure 13 The two different assemblies by Sumiya et al. (1996).

It is the author's opinion, that the usage of an effigy leg is important in order to reflect the behavior of the orthosis while worn by the patient. Nevertheless, plaster models are unable to reproduce the mechanical properties and the stiffness of the human limbs. Furthermore, while the foot is dorsiflexed/plantarflexed the AFO slides along the shank. If the effigy leg is made out of a rough material, then the friction between the leg and the AFO will hinder the deformation of the AFO. In this study, this obstacle was overcome by using a lubricant. The indirect loading of the AFO through the plaster foot and the lubricated calf region can sufficiently resemble the loading of the orthosis during ambulation. Despite the fact that the plaster model makes things easier is this experiment, more research needs to be conducted for the design of a model leg made out of foam and/or gels.

As it is mentioned in this report, the mechanical ankle axis does not match the anatomical axis. As most of the studies regarding the stiffness of the AFOs,

Sumiya et al. placed the ankle axis half way between the lateral and the medial malleolus (as shown in figure 14). Sumiya et al. supports this estimation: the talocrural and subtalar joints work mutually creating a “universal joint” between the shank and foot. Nevertheless, wearing an AFO prohibits the function of the subtalar joint letting only the talocrural joint to work. Thus the anatomical ankle joint in a patient wearing an AFO can be accurately reproduced by a hinge located in the axis passing through the lateral and medial malleolus.

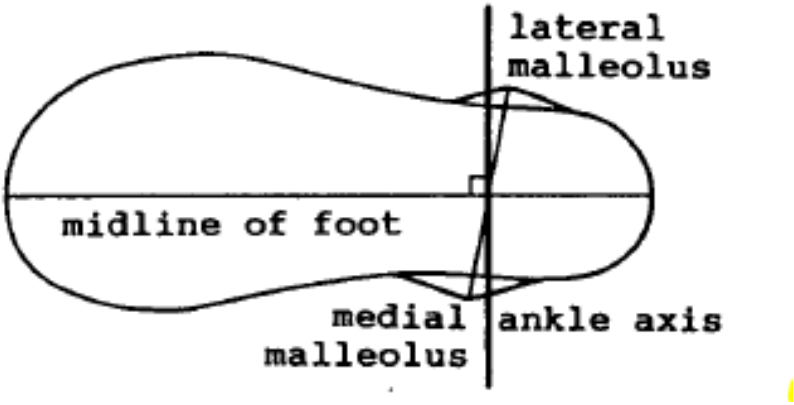

Figure 14 The location of the ankle joint (Sumiya et al., 1996).

The utmost moment generated manually with this device (with the loadshaft located 0.5m from the ankle joint) was 40Nm. Generally, based on published data (Klasson et al., 1998; Novacheck et al., 1998; Singerman et al., 1999) a 40 Nm moment is adequate to fully flex a polypropylene AFO to a degree that fully simulates the whole range of ankle motion of a patient wearing an orthosis. Nevertheless, AFOs with carbon inserts (Major et al., 2004), AFOs made of high-viscosity materials and AFOs produced from a thick polypropylene sheet (more than 4mm thick) require a larger moment in order to deform them in a similar way (e.g. according to Major et.al, an AFO with carbon inserts requires a 60 Nm moment in order to dorsiflex it by 14°). In order to apply a larger moment, the load shaft must be placed over 0.5m away from the ankle joint. Here lays one difficulty concerning

the operation of the device: as the loadshaft is elongated from the rotation center in order for the experimenter to apply a larger moment, the application of a small moment becomes more challenging since an error in the manual application of the force will be multiplied by the moment arm.

Despite the fact that the device is very simple and it can be probably used for clinical trials, the measurement is potential open to errors due to the manual application of the load. Sumiya et al. (1996) managed to overcome the difficulties about the position and the direction of the force: the two metallic bars and the tensiometer can guarantee that the force is always applied perpendicularly to the angle joint and therefore the moment applied in the AFO is accurately calculated. Nonetheless, in order for the operator to measure the stiffness of the orthosis, the readings from the tensiometer's screen and the AFO's deformation angle shown in the protractor must be accurately recorded at the same instant. Hence, the operator must be fully familiar with measurement method in order to acquire reliable measurements.

In this report, in order to confirm measurement reproducibility, the authors performed 400 repetitive tests, with appropriate relaxation intervals between them (the duration of those intervals is not given in this study), during which the experimenter was testing the moment reproducibility throughout the measurements. In plain English, the experimenter was asked to generate a specific moment to the AFO and then by manually pulling the tensiometer he tried to apply a moment as close as possible to the desired one. This procedure was repeated 400 times. Then the ratio of one standard deviation to the mean value was used as in indicator. The results have demonstrated very high reproducibility by the apparatus. Nevertheless, if the measurement in not performed by the same operator at all times, the reproducibility of the method is questionable.

Another important feature of the device is the usage of a vice in order to keep the model in a horizontal position. In this way, moments around the ankle joint generated by the mass of different parts are not effecting the measurement.

In conclusion, this model is cost efficient, easy to build, portable and with high reproducibility; also no computer/software is required for the testing. The device can mimic reasonably well the loading during gait, but further research is required in the manufacturing of the effigy leg. The accuracy of the measurement depends on the expertise of the operator; a larger moment is hard to apply without compromising the accurate application of a smaller moment, and vice versa. The test is destructive for the AFO since holes are drilled in the sole of the orthosis, but due to its simplicity it might be used in a clinical environment. The test is static, and the apparatus in not appropriate for cyclic and dynamic testing without any major mechanical alterations. No information was given regarding the fixation and alignment procedure of the AFO to the device.

In view of the fact that the biggest flaw in this measuring method lies in the accurate application of the force by the operator, one possible improvement would utilize some masses hanging by a thread from a pulley while the other edge of the thread is connected with the 4^{th} metallic bar (as a replacement of the tensiometer); if the mounting of the pulley allows one degree of freedom (moving left and right) then by moving the pulley, the operator can fix the thread perpendicularly to the metallic bar by using a second protractor. The rest of the model remains unchanged.

2.3.3 Bending test by Ross et al. (1999).

Ross et al. adopted a simple method in order to evaluate the bending stiffness of AFOs made out of various colours of polypropylene. During the test, each AFO was attached with 3 bolts (number 1 in figure 15) to a vertical bracket. Two holes were drilled in series on the mid-line of the AFOs' calf region, close to the proximal edge; a dial gauge (number 2) was clamped in the distal hole while masses (number 3) were hanging from the proximal hole. Two different configurations, with the AFO inverted and re-attached to the wall, allowed the application of plantarflexion and dorsiflexion moments.

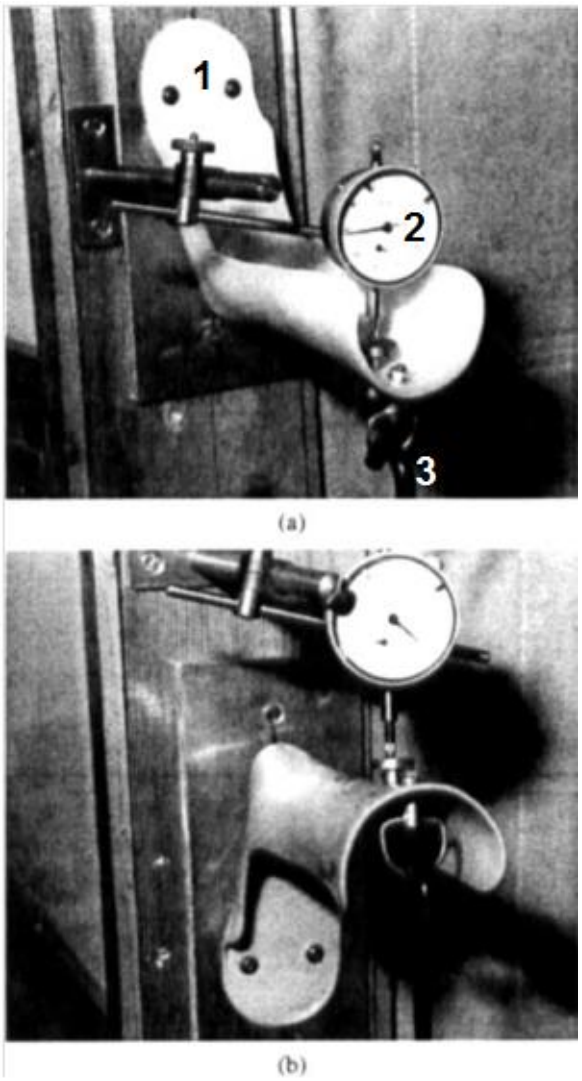

Figure 15 a) Plantarflexion and b) Dorsiflexion test (modified) by Ross et al. (1999).

All the AFOs were vacuum moulded over identical plaster casts; the AFOs' trimlines were made over the same markings in the cast allowing straight comparison. The thicknesses of the AFOs' were measured with a micrometer and the thickness variation of different areas is given to the report. A fine procedure was adopted in order for the holes to be transferred in every AFO. A shell made out of acrylic resin was laminated over an AFO. Then, 3x5mm holes were drilled in the sole of the shell and 2 more holes (with diameter of 3mm and 5mm) were drilled on the mid line of the calf region, at 30mm and 20mm from the proximal end of the AFO. After that, the resin shell was fitted to all 6 AFOs and the holes were

transferred in all of them. The 3 holes in the sole were used in order for the AFOs to be fixed in a metallic plate in a vertical wall. The 3mm hole in the calf region allowed the fixation of a dial gauge whereas a hanger for the masses was attached in the last 5mm hole.

Despite the fact that this set procedure for the fixation of the AFOs is very reliable, doubts arise over the location of the holes in the sole of the AFO. A careful examination of figure 15 reveals the location of the 2x5mm holes in the anterior part of the sole and the 2 holes in the calf region. No further information is given about the 3rd hole in the sole. The same figure suggests that this residual hole/bolt should be located anywhere in the posterior part of the sole. The position of this bolt is of major importance, especially during the dorsiflexion test, since this bolt determines the pivot point of the AFO. In figure 16, two different hole positions were assumed (a and b). Throughout the dorsiflexion test, if the aforementioned bolt is located at the point a, then the whole sole of the AFO will be in full contact during the application of the load. However, if the bolt is located at the point b, then the posterior part of the sole will rotate about that point.

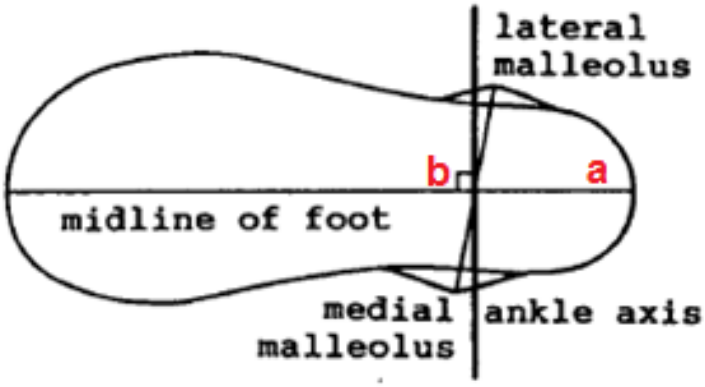

Figure 16 Bolt positioning (modified) by Ross et al., (1999).

Likewise, during the dorsiflexion test, in the second scenario where the bolt is located at the point b, the AFO's calf will be bended further than the first case

scenario (point a) and thus the displacement measured in the dial gauge will differ between those two cases.

The right positioning of the bolts in the sole of the AFO is debatable. Nevertheless, in each case, the proper calculation of the moment arm (indicated with a double black arrow in the next figure) is essential. In this study, no direct information is given about this distance; although, inspecting the results suggests that the moment arm was constant and equal to 0.173m. As mentioned before in chapter 2.3.2. Mechanical testing machine (Instron, model 1185), the assumption of a constant moment arm could lead to inaccuracies.

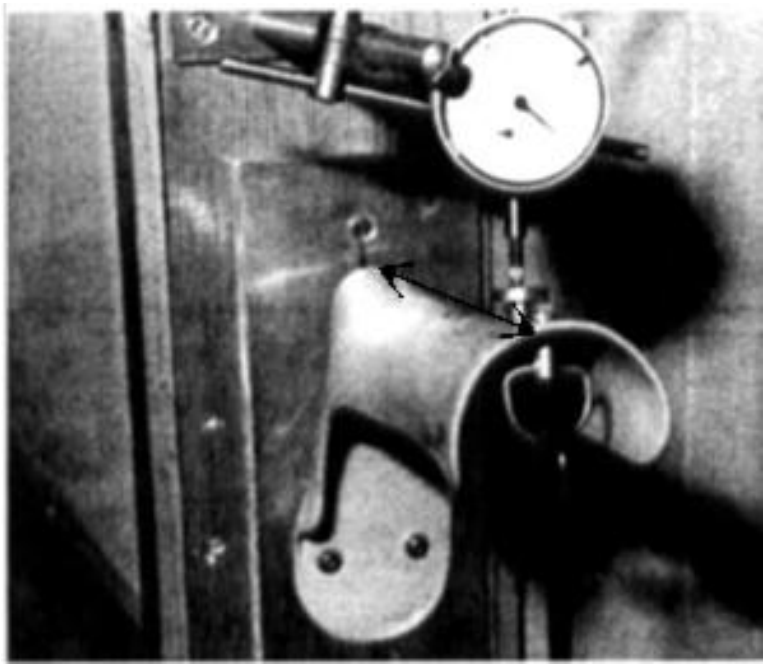

Figure 17 The moment arm used in the test by Ross et al. (1999).

In this study Ross et al. concluded that the colour additive in the polypropylene may alter the stiffness of the AFO. The next figure demonstrates the bending stiffness of 6 different coloured AFOs with the same trimline. Due to selection of the dial gauge as a transducer, in this study the bending stiffness is defined as the moment around the ankle joint (about which point the moment is measured is inconclusive in this report) per deflection (mm) of the proximal end of

the AFO. Those results can be translated with simple geometrical equations as moment per degree of ankle joint rotation in order to match results from other reports but this process of calculation is error-prone and more analytical methodologies can be tedious.

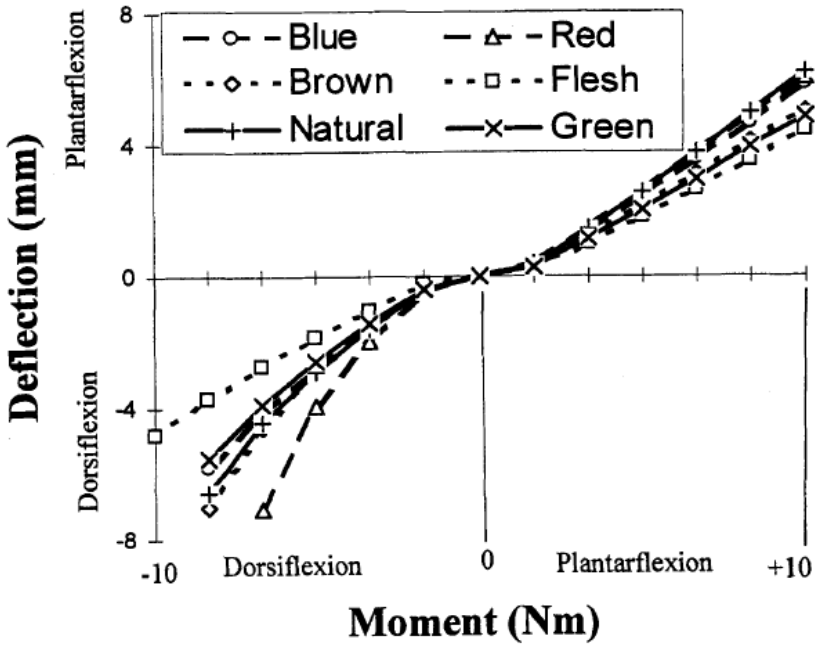

Figure 18 Bending stiffness of 6 coloured AFOs reported by Ross et al. (1999).

In conclusion this model can provide very accurate and reliable results in a comparison study. The fixation procedure can guarantee the repeatability of the testing method. Due to the nature of the transducer, the testing can only be static. The configuration is easy to build and easy to reproduce while the parts are cost-effective. On the other hand, the loading of the AFO is inconsistent with the loading pattern during ambulation while the absence of an artificial limb reduces the stiffness of the orthosis and facilitates the appearance of buckling due to the lack of internal support. The ease of use of this method is enhanced by the lack of any software or complicated mathematical model for the data analysis. One of the major problems of this method lies on the development of the acrylic resin shell: if

different types of AFOs or AFOs with different trimlines are to be tested, then a laminated shell should be made for each type of AFO. Thus, this stiffness determining method should be used only for direct comparison of AFOs of the same type and with the same trimline. Finally, difficulties may occur during the comparison of the results with other studies due to the diversity of the stiffness definition.

2.3.4 Automated device by Kobayashi et al. (2010).

Kobayashi et al. designed an automated apparatus, utilizing a non-destructive fixation procedure, and able to take dynamic stiffness measurements from an articulated ankle-foot orthosis (AAFO). It is beyond the scope of this thesis to examine methods for determining stiffness of non-solid ankle-foot orthoses; nonetheless, the design of this device is unique among the other testing machines described in the literature and it may be used in a testing with solid ankle-foot orthoses after certain modifications.

Figure 19 demonstrates the configuration of the device. The rod of the hydraulic servo fatigue testing machine was coupled with a rack in a manner that the rack-pinion pairing will convert the linear motion generated by the testing machine into rotational motion. The rotating axis of the pinion is connected with a torque meter and a rotary plate. The linear motion of the rod will force the rotary plate to move like a swing. By changing the frequency of the rod, the angular velocity of the “swing” can be adjusted. In a similar manner, changing the range of motion of the rod (the amplitude of the linear motion) will affect the range of rotation of the plate (the degrees of dorsiflexion/plantarflexion). A potentiometer is linked with a coupling and fixed next to the rotary plate.

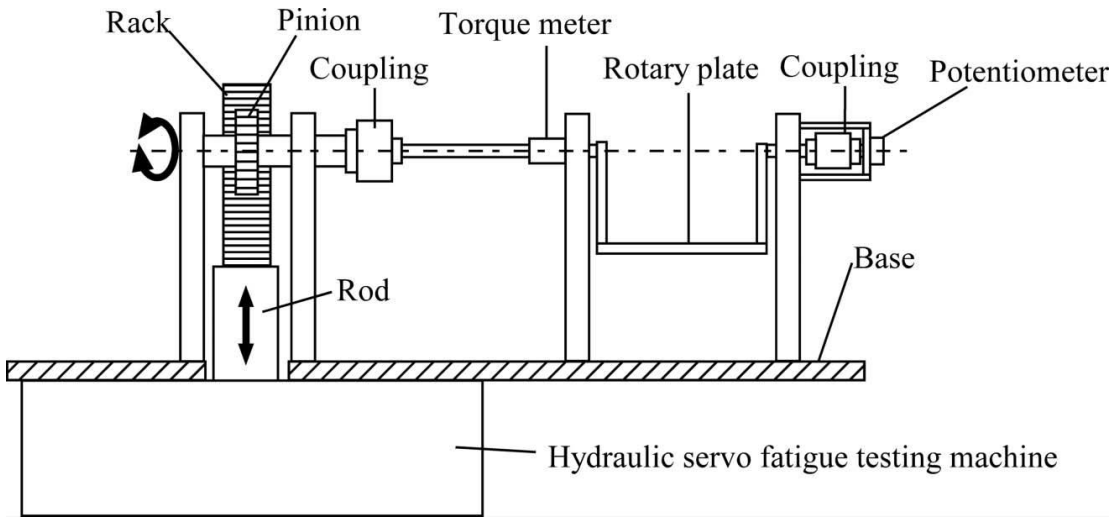

Figure 19 Automated AAFO stiffness measurement device by Kobayashi et al. (2010).

The AAFO was clamped in the rotary plate with a G-clamp. No further information is given in this report about the alignment and the fixation procedure followed in the testing. The rotational centre of the AAFO was assumed to be in the middle of the distance between the two ankle joints. Then the AAFO was positioned in such a way that the rotation axis of the plate would coincide with the rotational centre of the AAFO. The AAFO was fixed with the strap in an effigy shank. This shank was made out of plaster and a metallic pylon penetrating the plaster model was fixed in the supporter (figure 20). The hydraulic servo fatigue testing machine was tuned in such a way that the range of deformation was from -15° to 15° of dorsiflexion with an angular velocity of 10°/s. The output signal of the torque meter was fed into a computer for the calculations of the stiffness curve. The potentiometer was connected with an A/D converter and it is assumed that it was used for the calculation of the angles and the angular velocity.

As is can be seen by the following figure, the rotary plate is made out of two solid metallic arms and a metallic plate and there is no possible way to alter the radius of rotation unless shorter/longer arms are attached to the rotary plate. Hence, this particular configuration can be only used for only one type/size of AAFO as otherwise the rotational centre of the AAFO will not agree with the rotational

axis of the rotary plate. Therefore, here lies an imperfection since the design at the current stage doesn't allow a straightforward fixation of dissimilar AAFOs.

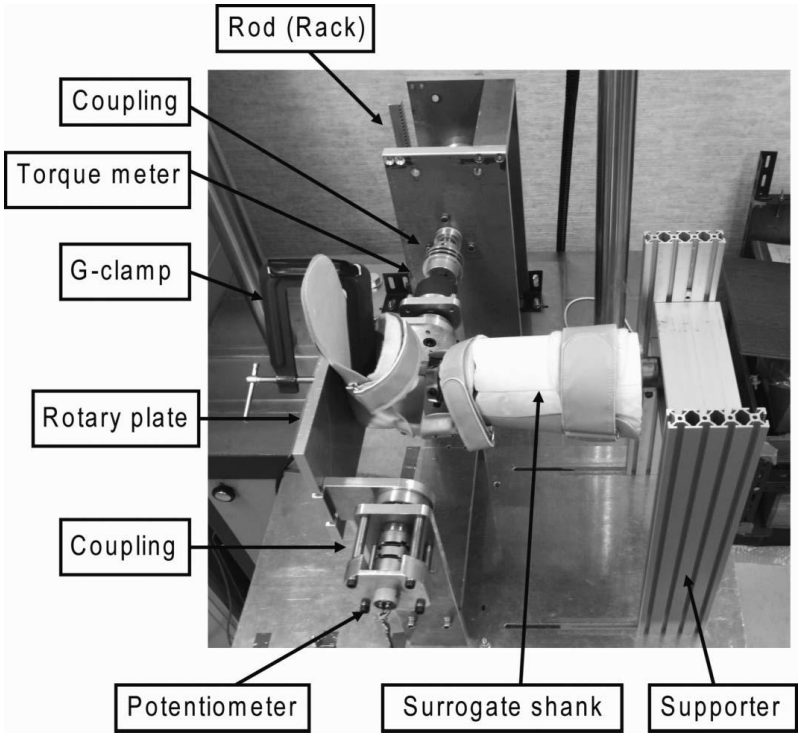

Figure 20 Automated AAFO stiffness measurement device by Kobayashi et al. (II)

This particular design cannot be easily used for solid AFOs stiffness measurements for three reasons. Firstly, it is reported by the manufacturer that the particular torque meter utilized in this apparatus cannot be used for readings greater than 22 Nm. Many researchers (Sumiya et al., 1996; Yamamoto et al., 1993; Major et al., 2004) have reported moments generated by the AFO throughout the stiffness testing far greater than the 22Nm. Thus, a torque meter with a larger rated output should be used. Secondly, in this paper, Kobayashi et al. reported the maximum stiffness of the AAFO to be equal to 0.13 Nm/°; this stiffness is fairly small compared to the stiffness of a solid AFO (Sumiya et al., 1996; Yamamoto et al., 1993; Major et al., 2004). There is no information given in this report about the maximum torque that the fatigue testing machine connected to the rack/pinion can generate and if they are adequate for non-articulated AFO testing. Thirdly, the fixation with a G-clamp might be sufficient to hold the AAFO to the plate during a

testing where the maximum torque does not exceed 2Nm but it is uncertain that it can effectively hold a solid AFO during a similar experiment.

In conclusion, this design is not indicated for solid-AFO stiffness measurements. The major drawback is the inability of the rotary plate to fit any AFO without the arms to be readjusted. The loading pattern can satisfactorily mimic the patient's ambulation. The loading of the AFO is similar to the one achieved by Sumiya et al. (chapter 2.3.2); the main difference between the two approaches is that the loading in the apparatus designed by Sumiya et al. is applied indirectly to the AFO thought the plaster foot whereas in the automated design by Kobayashi et al. the loading is applied from the rotating "ground". The main advantage of this design is that the operator can perform controlled dynamic tests instead of static measurements (Sumiya et al.) while the operation bias is eliminated. Errors may only originate from the measurement devices (torque meter and potentiometer) and from the imprecise fixation protocol.

2.3.5 Dynamic AFO testing apparatus by Lunsford et al. (1994).

Lunsford et al. designed a device in order to quantify the stiffness and the buckling of pediatric AFOs during cycling loading. The mechanical properties of the orthosis were measured during a 72-hour loading cycle. The orthosis used was a pediatric Rancho-type, polypropylene, solid-AFO described in the manual: Rancho-type polyproplylene AFO fabrication manual (Lunsford T., 1982). The aforementioned manual is cited in two reports related to AFO stiffness (Singerman, Hoy and Mansour, 1999; Lunsford, Ramm and Miller, 1994) but a thorough search revealed that this publication is not available online and it is locally accessible at the Rancho Los Amigos National Rehabilitation Center based in Downey, California.

In this study a unique and interesting approach on the design of the AFO and the surrogate leg was followed. The effigy leg (30.5 cm height) was moulded based on a 10-year-old-male patient. The limb was made out of polyester resin and it was fully covered by a nylon stockinette. Compared with other studies using a plaster

leg (Sumiya et al., 1996; Kobayashi et al., 2011) the resin surrogate leg is less stiff and more compatible with the human limb. Furthermore, it is assumed that the nylon stockinette was utilized in order to create a soft contact area between the AFO and the surrogate limb and consequently minimizing the friction during the test while allowing the limb to naturally slide over the orthosis. It seems that the polyester limb is the most fitting solution for a cycling test: the most plausible scenario is that a plaster leg would fail due to fatigue in a 72-hours testing. Similar to the effigy leg by Sumiya et al., this design contains a free-motion mechanical talocrural joint. This joint was placed 6cm proximal to the plantar surface and 5cm anterior the posterior coronal plane (figure 21). The AFO was moulded based on the effigy leg and not the other way around as it usually happens in similar experiments. That way, the standard prescription procedure was followed and the harmonizing of the leg/AFO was guaranteed. Finally, a straight perpendicular line passing from the ankle joint of the effigy leg was drawn in order to assist the measurement of the stiffness of the AFO.

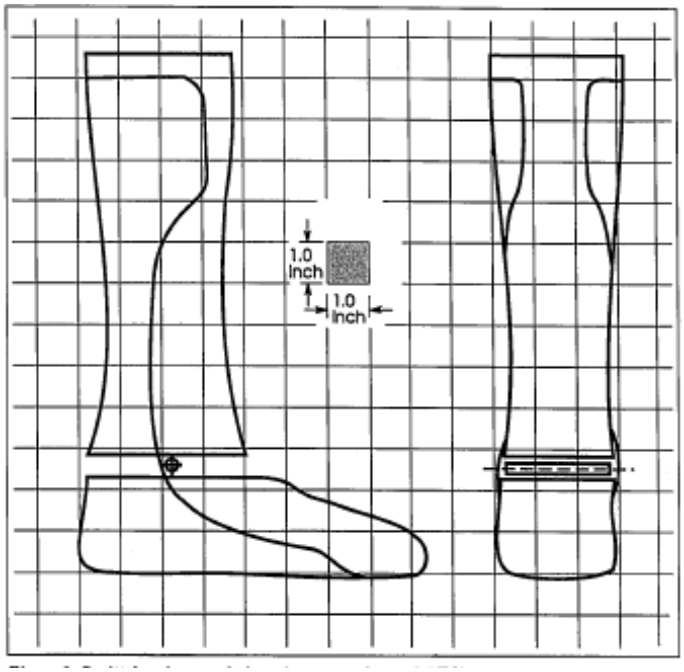

Figure 21 Graphical representation of the leg and the AFO's trimlines by Lunsford et al. (1994).

The automated cycling device was composed out of a metallic frame (number 1 in figure 22), an electro-motor (No 2), a pulley (No 3) and a crank/rod (No 4). The motor will rotate the pulley forcing the rod to move back and forth and parallel to the ground. The AFO/surrogate limb (No 5) was *mounted* in the device and a protractor (No 6) was placed next to the ankle joint in order to measure the angle of deformation. No further information is given about the mounding procedure. However, based on the figures in the report, it is assumed that the AFO was clamped instead of drilled. As shown in the figure, the AFO is mounted on a metallic base. Probably, the positioning of the frame was used in order to adjust the angles of deformation: since the rod is moving by a fixed distance, altering the distance between the ankle and the edge of the rod will obviously change the deformation angles while by moving the frame, the neutral angle can be selected. The cycling was continuous from 10° of dorsiflexion to 15° of plantarflexion.

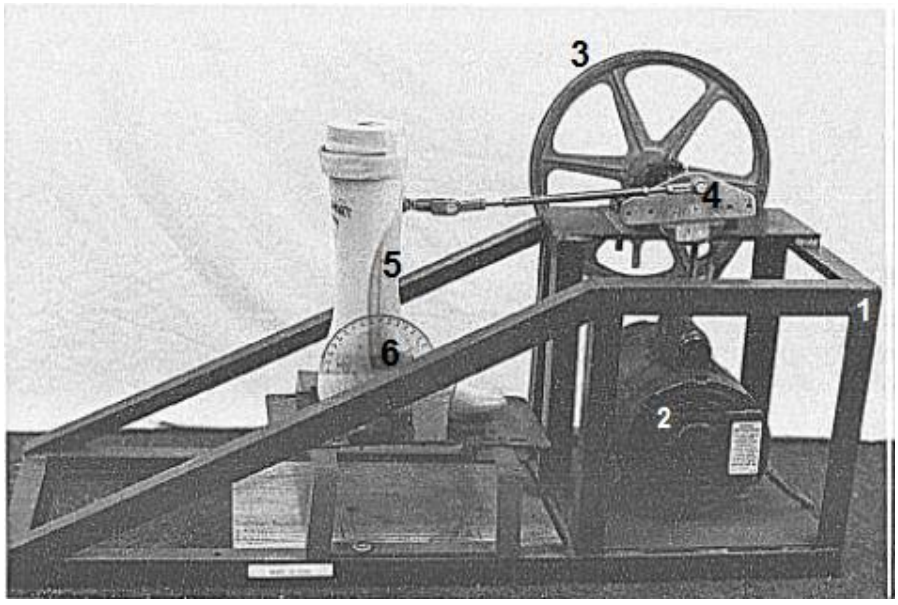

Figure 22 Dynamic AFO testing machine (modified) by Lunsford et al. (1994).

Clearly, the repeatability and the accuracy of the rod's motion are dubious and thus the AFO's angle of deformation during the cycling loading is open to an error. Nevertheless, a deviation in the plantarflexion and dorsiflexion angles in a 72-hours experiment is expected and its influence in the results is negligible.

In this report, the stiffness of the AFO is defined *as the force needed to cause 10° of dorsiflexion*. The stiffness of the AFO was measured prior to the experiment and every 24 hour thereafter. For the measurement to take place, the electro-motor was stopped, the rod was detached from the pulley and a force dial was connected to the rod. Then, the operator pulled the force gauge until the AFO was deformed from 0° to 10° of dorsiflexion. The angle of the deformation was measured with a protractor. Three measurements were recorded on every occasion and the mean force value was documented as the *force.*

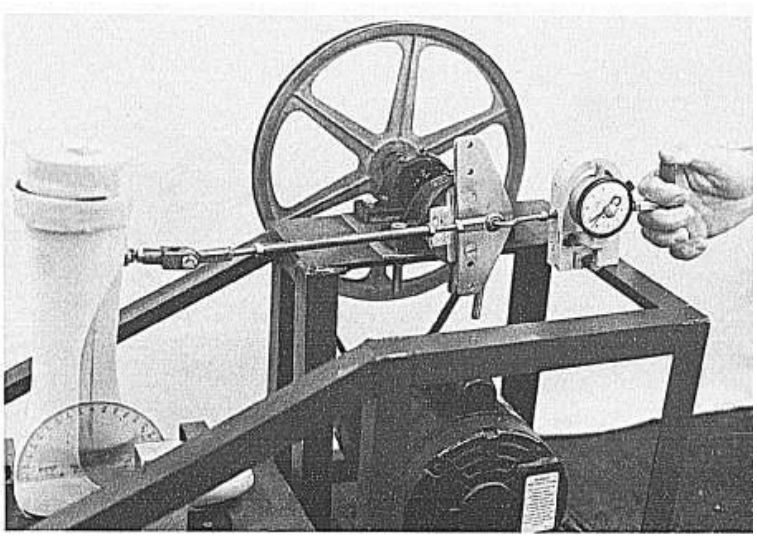

Figure 23 The stiffness measurement as performed by Lundsford et al. (1994)

This measurement approach is deficient in several respects. Compared to the digital tensiometer used in the study by Sumiya et al. (1996), the force gauge is inaccurate and the measurement is open to a considerable operation error: It is reported that the *force* required to collapse the AFO prior to the experiment was 366N which is an appreciably large force to apply manually. Furthermore, this configuration allows only the measurement of the stiffness during dorsiflexion. In order for a plantarflexion measurement, the force gauge must be placed in the opposite side and possibly a hole must be drilled in the AFO for the application of the force. The contribution of the leg's weight to the force (the component of the weight while the AFO is dorsiflexed) is considered negligible compared to 366N that

were applied during the test. Nevertheless, such an experiment is preferred to be carried in the plane parallel to the ground.

Concerning the simplicity of the approach, this experiment resembles the stiffness measurement by Ross et al. (figure 24). Ross et al. applied the force by hanging masses to the calf of the AFO while the displacement was measured with a dial gauge. The main difference between the two approaches is the presence of an effigy limb throughout the experiment. In the stiffness measurement by Ross et al. the AFO will elastically deform (the calf will bend due to the masses hanging). To some extent, this deformation will alter the moment arm and thus utilizing simple geometrical equations such as the Pythagorean Theorem to measure the moment and the deformation angle of the ankle joint is doubtful. On the other hand, introducing a stiff dummy leg will, apart from changing the stiffness of the AFO in order to better resemble the human leg/AFO, will prevent the AFO to elastically deform under the load and thus rendering the usage of simple equations more reasonable.

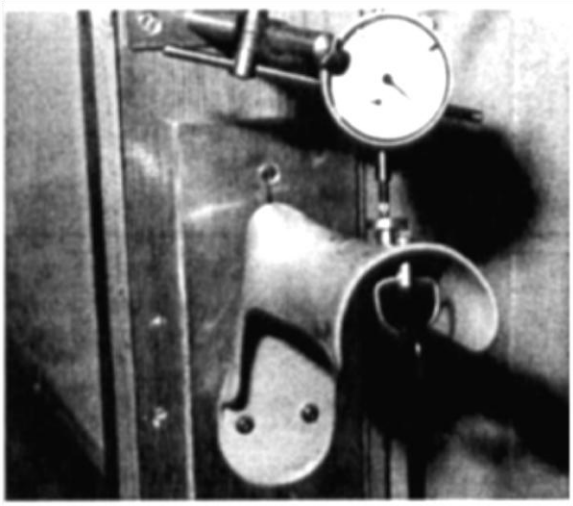

Figure 24 The stiffness measurement as performed by Ross et al. (1999).

Despite the minimalism of this stiffness-determining method, this study reported some very interesting results about the viscoelastic properties of the AFO on fatigue testing. Prior to the cyclic loading, the required force in order to dorsiflex

the AFO by 10° was 366N (36.6 N/degrees). After 24 hours of loading the stiffness was recorded equal to 25.4 N/degrees, after 48 hours 23.9 N/degrees and after 72 hours 23.7 N/degrees. Clearly, regardless of the accuracy of the measurement method, the AFO stiffness was notably reduced after the first 24-hours testing and considerably less in the next two periods. Nevertheless, after the testing, the orthosis was allowed to rest and the stiffness was improved by 23% from 23.7 to 29.2 N/degrees. After a full hour rest, the AFO's viscoelastic properties were fully recovered. Clinically, if the patient succeeds to stress an orthosis to this point, the deterioration of the AFO's stiffness might affect the efficiency of the orthosis. Despite that, even a 15 minutes rest is sufficient in order for the AFO to recover.

2.3.6 Test apparatus by Klasson et al. (1998).

In this report, Klasson et al. designed a testing device to measure the stiffness of AFOs in other planes than the one that the orthosis is loaded. During the manufacturing of the orthoses, a master plaster model was used to mould the AFOs (number 1 in figure 25) and a calf model. A long rod was pinned through the malleoli of the master model in order for orthotist to accurately transfer the ankle axis to all the ankle-foot orthoses and to the dummy calf. The dummy calf was made out of a metallic cross-sectional column (number 2) that was covered by polyurethane foam (number 3). This metallic column was located vertically over the ankle axis that was defined by the long rod pinned in the master mode. Holes were drilled proximately to the metallic column and four outriggers were placed in these holes (numbers i, ii, iii, iv). Similar holes were drilled distally in the calf model. After fitting the dummy calf in the AFO with Velcro straps, a long pin with a hot tip was passed through the distal holes and throughout the AFO. The hot tip was removed and four more outriggers were screwed in the metallic column of the dummy leg (numbers v, vi, vii, viii). Those eight outriggers were later used for the application of the loads. Furthermore, in the proximal and distal outriggers (numbers ii, iii, vi, viii) two aluminum plates were attached (numbers 4 and 5). Those two plates were used in order to define the sagittal and the coronal plane when the AFO was unloaded.

Finally, three holes were drilled in the sole of the AFO for the proper fixation of the orthosis to the testing apparatus. No information was given about the dimensions of the bolts.

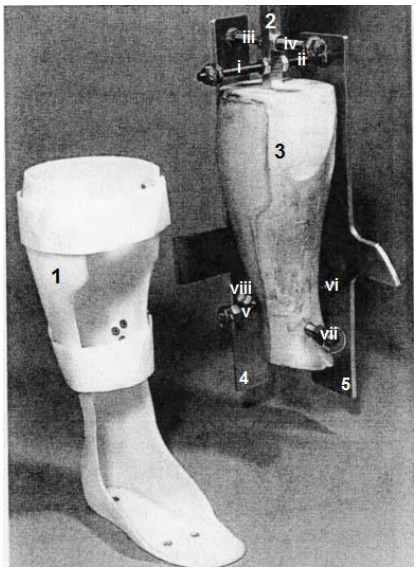

Figure 25 AFO and dummy calf (modified) by Klasson et al. (1998).

The test apparatus was constructed out of two metallic cubical frameworks, one inside the other. Six dial gauges were attached to the inner framework in a way that when the AFO is fixed in the device, the tips of the dial gauges will be in contact with the two aluminum plates (figure 26).

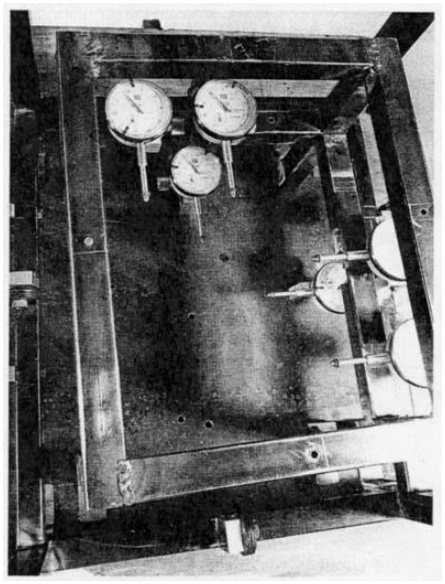

Figure 26 The testing apparatus by Klasson et al. (1998).

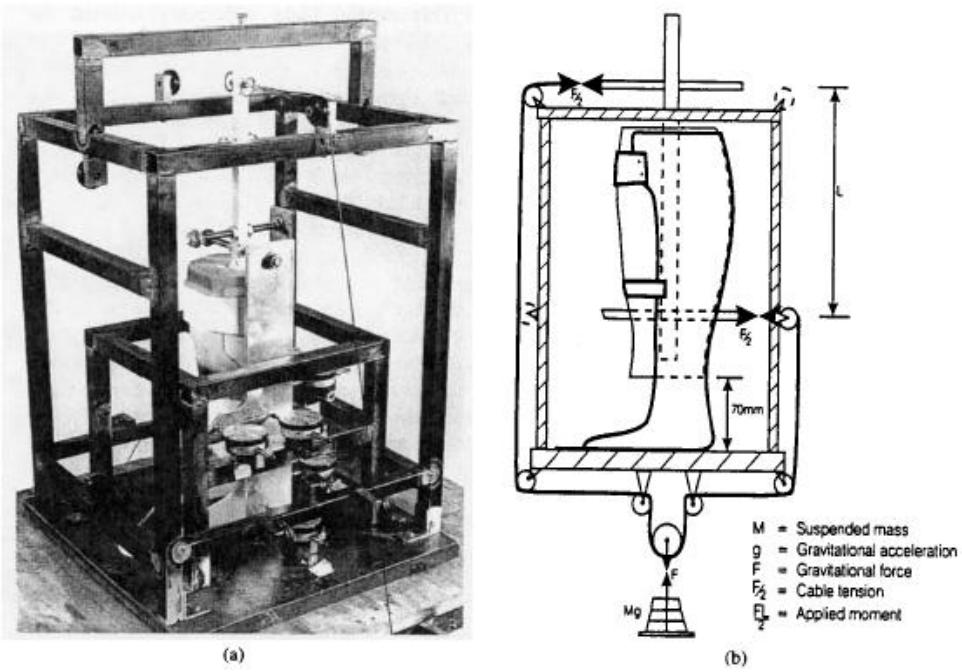

Figure 27 The testing configuration by Klasson et al. (1998).

Hooks were attached to the proximal and distal outriggers of the metallic column. A single cable passing over pulleys was attached to those hooks while masses were suspended beneath the apparatus, as shown in figure 27 entitled “The testing configuration by Klasson et al. (1998”. The philosophy of this configuration is that a pair of forces applied via the cables will produce two external moments, while the dial gauges attached to the aluminum plates will record translations and angulations of the AFO.

The dial gauges are able to measure two linear and three rotational movements. Out of the six degrees of freedom only the translation in the Y axis cannot be measured. Plantarflexion and dorsiflexion can be measured by the simultaneous recordings of the higher and lower dial gauge in the aluminum plate defining the coronal plate. Respectively, the two dial gauges in the other plate can measure inversion and eversion. All three rotations can be measured by combining the recordings of two dial gauges in the same plate.

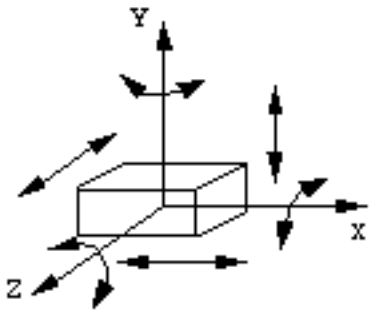

Figure 28 The six degrees of freedom

The major advantage of this technique is the capability of the apparatus to measure the flexibility of the AFO in different planes. Those measurements are of great importance since the AFO is loaded in all the planes during patient's ambulation. Furthermore, Chowaniec (1983) reported that during the application of the inversion/eversion loads, a deformation in the sagittal plane was recorded by the strain gauges. Also, in this report, Klasson et al. reported that the application of moments in the sagittal plane results in translations and angulations in all the planes. In figure 29, the dotted line shows the location of the aluminum plate in the coronal plane before loading while the solid line shows the position of the plate during constant loading. As it was mentioned in this report, the center of rotation of the dummy calf is located in the ground (the radius of rotation depends on the load applied during the test) and thus it cannot coincide with the ankle joint. Certainly, the translations in the X and Z axis are due to the lack of an ankle joint. The absence of the joint hinders the potential of this method to mimic the loading during normal gait since during the stance phase the tibia can only rotate around the ankle joint.

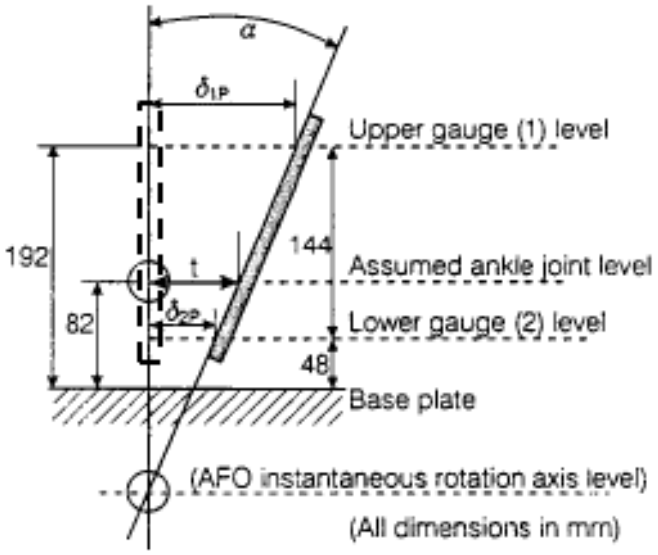

Figure 29 Translation of the coronal plate (modified) by Klasson et al. (1998).

As mentioned in this report, the recordings of the dial gauges cannot be all read at the same time; the operator must record every reading individually and therefore this measuring method is sensitive to creep. Furthermore, the dial gauges can only measure statically and not continuously and thus the system must reach equilibrium in order for the operator to record the translations. Despite that, repeating the experiment with ascending and descending masses can lead to accurate stiffness diagrams throughout a range of moments that correspond to those that apply during gait.

In this report, simple geometrical equations are presented for the calculation of angles and translations. Nevertheless, no information is given about the calculation of the moments. This negligence raise questions about the calculation of the moment arms and the forces generated by the tension in the cable: when the AFO is not loaded the cable between positions a-b and c-d is parallel to the ground (figure 30). But when the AFO is loaded the metallic column passing through the calf is translated and rotated. Thus, after loading, the cable connecting the pulley and the column is not any more in parallel to ground and thus the direction of the forces

is shifted while the amplitude of the forces is not equal any more to M*g/2. Of course, if the geometry of the apparatus is known, those forces and the ground reaction forces can be calculated. Nonetheless, there is no information given about the dimensions of the apparatus and the weight of the dummy calf. Finally, it is not clear if the moment reported in this paper corresponds only to the external moments generated by the cable or if the ground reaction forces and mass of the dummy leg are included. That information is important for the reproductivity and the verification of the results presented in this study.

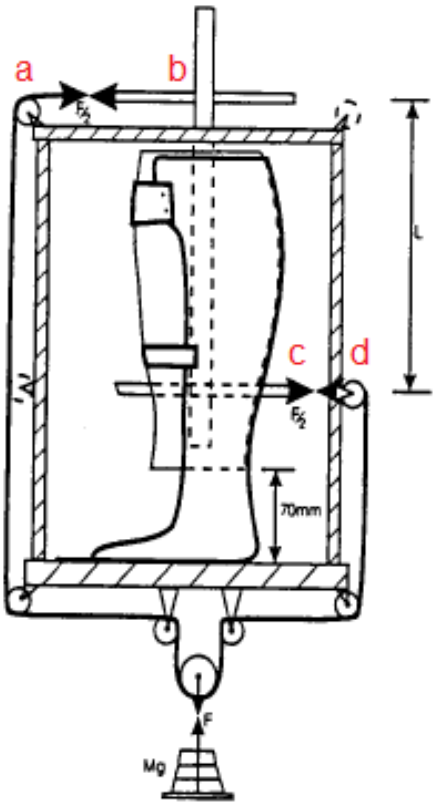

Figure 30 The test aparatus (modified) (b) by Klasson et al. (1998).

In conclusion this method provides a fine but complicated way to determine the stiffness of ankle-foot orthoses in other planes than the loaded one. Despite the fact that the device is cost efficient, it is not easy to build and most likely it is not efficient for clinical testing. Even though there is no need of software to analyse the

data, the calculation of the moments and the displacements in all three planes could be challenging and time consuming.

2.3.7 AFO testing machine by Cappa et al. (2003).

Cappa et al. developed an AFO testing apparatus capable of evaluating the stiffness of an orthosis in a 2-D manner. This device, along with the one designed by Klasson et al., are the only two devices in the literature that are able to perform stiffness measurements in more than one planes. Both devices have increased design and set-up complexity; nevertheless their results are reliable and their testing procedure is applicable in clinical testing.

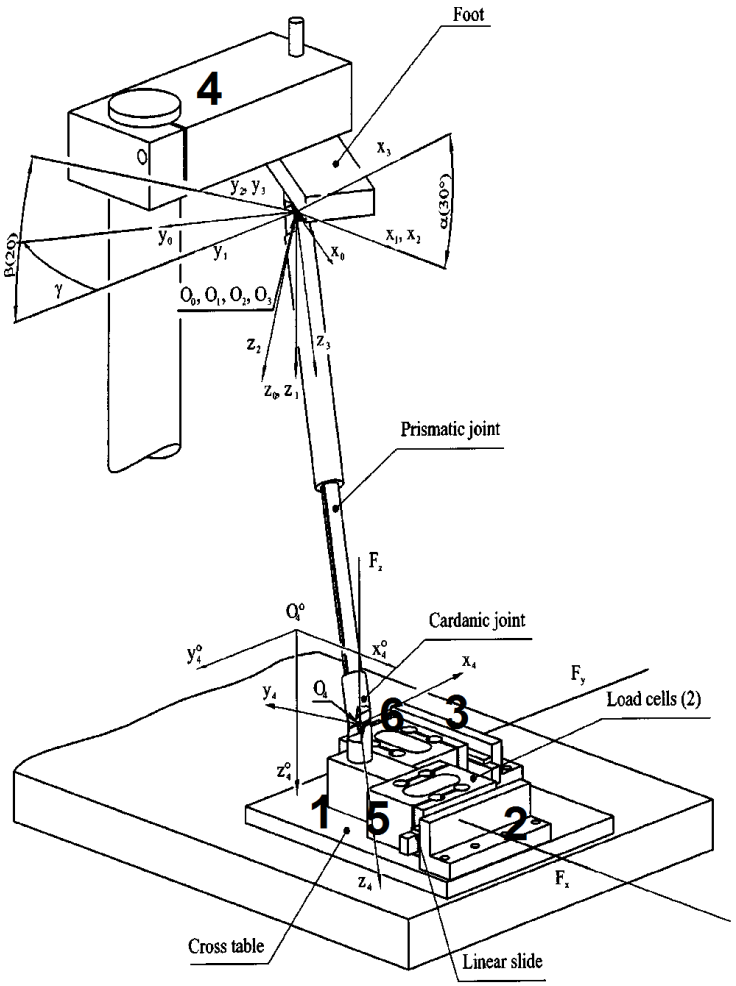

Figure 31 The design (modified) by Cappa et al. (2003).

The stiffness testing apparatus is constructed with off-the-shelf machine elements: a cross table (number 1 in figure 31), two slides (number 2 and 3), and a metallic frame (number 4). The effigy leg (which is reversed in this design i.e. the foot is over the shank) was composed out of a cardanic joint and a prismatic joint. The prismatic joint (slider) was used to replicate the calf of the leg. The cardanic joint was enabling the movement of the shank only when then experimenter is sliding the two hand controlled slides (number 2 and 3).

For illustrative purposes a cardanic joint (or double universal joint) is shown in figure 32. The first joint (i) corresponds to the bottom joint of the effigy leg which is connected with the cross table. The second joint (ii) corresponds to the ankle joint. Part (iii) corresponds to the shank of the model and in this design it is replaced with a prismatic joint. With this configuration, when the experimenter is moving the two slides, the shank is able to move freely in space.

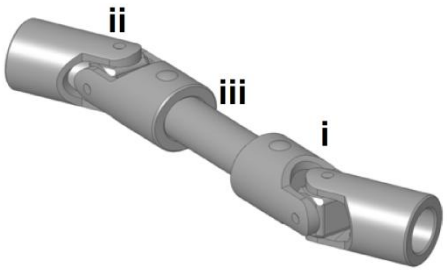

Figure 32 The cardanic joint (modified), (Commons.wikimedia.org, 2014).

The foot, which is a rigid metal plate, is firmly connected to the fixed metallic frame (number 4) with two small bolts. No information was given about the geometry of the bolts and the holes. When the operator moves the hand-controlled slides by a distance x and y, the dorsiflexion/plantarflexion angle (a) and the abduction/adduction angle (β) (as shown in the sketch of the apparatus) can be calculated with the following two formulas:

$$x = L\,\frac{\tan(\alpha)}{\cos(\beta)}$$

$$y = L\tan(\beta)$$

Where, L is the vertical constant distance between the two universal joints, when the prismatic joint is vertical in relation to the ground. Those distances x and y can be found with the assistance of an optoelectronic system: two screws in the sliders (2 and 3) are monitored by two incremental optical encoders. In order to measure the stiffness of the AFO, the reaction forces F(x) and F(y) are measured with two load cells on top of the cross table (number 5 and 6). Hence the moments in the sagittal M(α) and the frontal M(β) plane can be measured with the following formulas (the calculation of the moment's formula can be found on the appendix of the study):

$$M(\alpha) = -F(x)\,\frac{L}{cos^2(a)\cos(\beta)}$$

$$M(\beta) = \frac{L}{cos^2(\beta)}\,[F(x) - F(y)\tan(a)\sin(\beta)]$$

As mentioned in the report, this configuration fails to represent the natural orthosis/skin interface. Furthermore, in this study, only a spiral AFO was tested (no information were given about the mechanical characteristics and geometry of the used AFO). Due to the AFO selection, there are not any data available about the stiffness testing of a solid AFO and hence, no room for comparison of their results with other stiffness studies in the literature. Furthermore, the fixation of the spiral AFO raises questions: how did they fix the spiral AFO in the prismatic joint (e.g. the calf model)? It is practically impossible to fix the AFO using a Velcro strap without any rigid calf model with geometry close to a human limb. In addition, the motion of the prismatic joint will make the proper fixation of the AFO even harder.

As it mentioned in this study, the operator moves the two slides in order to move the effigy shank and therefore, to deform the spiral AFO. Hence, the load is applied manually. A spiral AFO is flexible enough in order for the experimenter to

perform this experiment by hand. It is questionable if the operator would be able to equally deform a fairly solid AFO i.e. a thick solid ankle-foot orthosis without any mechanical assistance.

In order to test the reliability of the testing methods, Cappa et al. used a hanging mass and applied a constant load at the point O1 equal to 29.4 N. After three trials, the load cells measurements had a standard deviation of the vector magnitude less than 2 N (i.e. 6.8%) and an error associated to the deformation angle less than 5°. Nevertheless, the reliability of this method is still doubtful; only three trials and a fairly small load, far less than the natural loading of the AFO during ambulation, cannot guarantee the reliability of the measurement. Also, the verification procedure must be repeated with increased loads in order to check the linearity of the error.

Figure 33 A Spiral AFO (Trulife.com, 2014).

In conclusion, Cappa et al. stiffness method is low-cost and fairly simple and allows the evaluation of the AFO stiffness in two dimensions. This configuration is easily applicable in clinical and industrial setting in order to allow the tailoring of an orthosis compatible with the unique needs of every patient. Nevertheless, the

reliability of the apparatus, the fixation protocol of the AFO in the calf model and the efficiency of the device with a non-spiral AFO is questionable.

2.3.8 Bruce method by Bregman et al. (2009).

Bregman et al. (2009) developed an AFO testing apparatus capable of evaluating the biomechanical characteristics of an ankle-foot orthosis. The device called BRUCE, which stands for Bi-articular Reciprocating Universal Compliance Estimator (Figure 34), is able to measure the stiffness around the ankle and the metatarsal joint and the neutral angle of the AFO. Moreover, the device is capable of estimating the stiffness of an ankle-foot orthosis when combined with a shoe.

The aluminum base of the device (number 1, figure 34) serves as a data acquisition box containing strain gauge amplifiers and a NI-DAQ digitizer. The acquisition box converts the signal coming from the transducers into a digital signal which is transferred to a computer via a USB. The sampling frequency is held constant and equal to 100Hz.

To ensure that a vast variety of AFOs could be measured, six different aluminum effigy feet with lengths from 175 to 300mm (number 2) were manufactured. The ankle and metatarsal axis location of the assembly is based on anthropomorphic data from 5000 tests at the James R. Gage Center for Gait and Motion Analysis (Bregman et al. 2009). The AFO is non-destructively secured in the effigy leg with two clamps.

The effigy leg (number 3), which is 45 cm in total, is composed out of two square metal tubes and two unidirectional hinges for the knee and the hip joint. Posterior of the effigy leg, a guiding prismatic joint (number 4) allows the hip joint to move only vertically. A spring inside the prismatic joint compensates for the mass of the dummy leg and the prismatic joint itself. In order to determine the stiffness of the AFO around the ankle joint, the experimenter can manually move up and down the upper shaft of the prismatic joint, forcing the effigy leg in flexion or extension (as shown in figure 34 by the arrow). A force transducer (LCDA-150,

Omega) is positioned 20 cm over the ankle axis whereas a potentiometer located in the ankle can measure the joint's angle throughout the test. Small rubber cushions under the effigy feet and a plastic spacer around the metallic leg can assist the proper fixation of the AFO in the effigy leg.

Moreover, for determining the stiffness of the AFO in the metatarsal joint, the forefoot plate can be manually lifted around the metatarsal axis. The flexion angle is measured with a potentiometer located in the joint axis. A force transducer (LCGB-250, Omega) located 100 mm posterior of the metatarsal joint axis is measuring the applied force. The data gathered from those two transducers can be used for the calculation of the moment and the stiffness around the metatarsal joint.

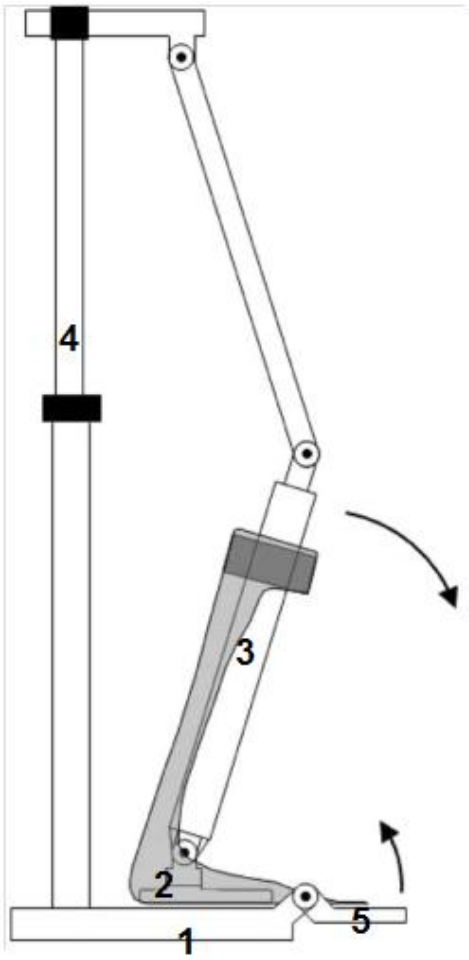

Figure 34 Overview of the Bruce (modified) by Bregman et al. (2009).

Throughout the experiments, the ankle joint motion was ranging from -10 to 20 degrees of dorsiflexion whereas the metatarsal joint from 0-30 degrees of flexion. Finally, it should be noted that the forefoot platform (number 5) can be rotated in the transverse plane from -30 to 30 degrees in order to mimic the loading of the AFO by patients with tibial torsion.

The author of this thesis believes that the spring inside the prismatic joint may alter the results obtained, especially during the unloading of the orthosis. During the dorsiflexion test, the spring will store energy while it is compressed. Throughout the plantarflexion test, i.e. when the operator lifts the hip joint, the spring will assist the unloading of the AFO changing the unloading rate of the test.

During the test, four AFOs were tested: two custom made carbon composite posterior leaf spring AFOs of different stiffness, one rigid custom made polypropylene AFO, and a medium size Dynafo posterior leaf spring AFO. The three custom-made AFOs were based on the cast of a healthy subject with a foot length of 25 cm. Each AFO was tested by three different operators. Each operator performed the measurement three times. After two days, the same experiment was repeated, giving eighteen measurements in total for each ankle-foot orthosis. Those results were used to determine the error caused by different factors. Those factors were the tester, the occasion (1st or 2nd day of the testing) and the repetition of the test (1st, 2nd and 3rd measurement). The variance caused by each of these three factors was found and it was reported that the tester was the aspect that caused mainly to the error variance. Thus, Bregman et al. suggested that a single tester should always perform all the measurements in order for this source of error to be neglected.

All in all, Bregman's et al. stiffness measuring method is simple and cost efficient and it is easily applied in clinical practice. It is not destructive for the AFO and it can be used for measuring the stiffness of the AFO around the metatarsal joint or the stiffness of the AFO combined with a shoe.

3 Stiffness testing

The study had the following objectives:

1. To fabricate and document an effigy leg suitable for the stiffness test of an AFO.
2. To measure and compare the stiffness of an AFO with the following methods:
    a. Testing the stiffness of an AFO, without using the dummy leg, in a material testing machine (Instron ElectroPuls 10000), following the method described by Major et al. (2004).
    b. Testing the stiffness of the AFO/effigy-leg assembly in the same material testing machine (Instron ElectroPuls 10000).
    c. Testing the stiffness of the AFO by using hanging masses, following the method reported by Ross et al. (1999) and Hagenbeek (2013).
    d. Testing the stiffness of the AFO/dummy-leg assembly following the aforementioned protocol (method c).

The results of this study can make a difference in the prescription and manufacturing of an AFO throwing light on blurred aspects of the methodology for determining the stiffness of ankle-foot orthoses. More precisely this study will report on:

I. Significance of using an effigy leg during the testing procedure: Comparing objectives a-d will highlight the influence of a dummy leg in the stiffness measurement of the AFO. By comparing these results with relevant data obtained from functional tests (i.e. tests with real patients), future studies will be able to manufacture effigy limbs that can resemble the human leg even more accurately and significantly improve the bench-testing protocols.

II. Difference in the results obtained from two different approaches: Those two methods (Major et al., 2004; Ross et al., 1999) were not randomly selected. Major's method is utilizing a material testing machine (Instron 1185), which is an extremely costly but also exceptionally accurate machinery; on the other hand, Ross et al., had used only hanging masses and a dial gauge to perform the same measurement. Thus, examining the objectives a-d will pinpoint the error between the two approaches, and highlight the most suitable protocol based on parameters such as the cost of the machinery used and the accuracy of the results.

3.1 Instron Electroplus 10000 testing

For the purposes of this study, an effigy leg was manufactured (figure 35). The effigy leg was modelled after the AFO that was used later on in this study. The leg consisted of a single-axis foot (9.5 UK size) whith a uniaxial ankle joint, a metallic tube, and a single- axis hinge for a knee joint serving as the upper mounting jig. The calf of the dummy leg was made out of polyurethane expanding Pedilen rigid foam, series 617H32 and 617P21 (OttoBock health care, USA, Plymouth). The hallow metallic tube was made from an aluminum alloy with a diameter equal to 30.1 mm, thickness equal to 2.25 mm and a total length equal to 450mm.

Figure 35 The effigy leg.

The single-axis foot and the uniaxial ankle joint are shown in figure 36 and figure 37 respectively. According to Ottobock “the single-axis feet are designed to quickly and efficiently reach a secure standing position. These feet are recommended for low-activity amputees who are primarily indoor walkers” (Professionals.ottobockus.com, 2014). The total mass of the effigy leg was equal to 1.65Kg.

Figure 36 A single-axis foot by Ottobock (not the one used).

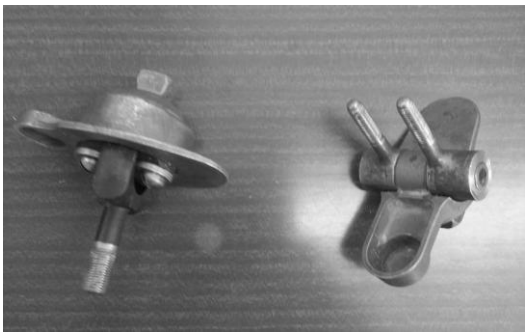

Figure 37 Uniaxial ankle Joints.

Three AFOs were tested in total: a 4.6 mm black co-polymer solid AFO, a 6mm homo-polymer solid AFO and a 4.6 co-polymer AFO with carbon fibre shape corrugations. The AFOs were modelled after a healthy male individual. Two Velcro straps, one over the calf of the AFO and one over the malleoli region were used. Prior to the test, a shoe (13 UK size) was worn in every AFO and both the AFO and the shoe were secured with four 3mm bolts in a wooden plate. The wooden plate

(120x60x20mm) was able to rotate over the lower mounting jig. The whole assembly was mounted in a metallic base allowing the proper fixation of the ankle-foot orthosis to the Instron 10000. Finally, the dummy leg was placed in the orthosis; only the Velcro straps and the shoelaces were used for the fixation of the leg.

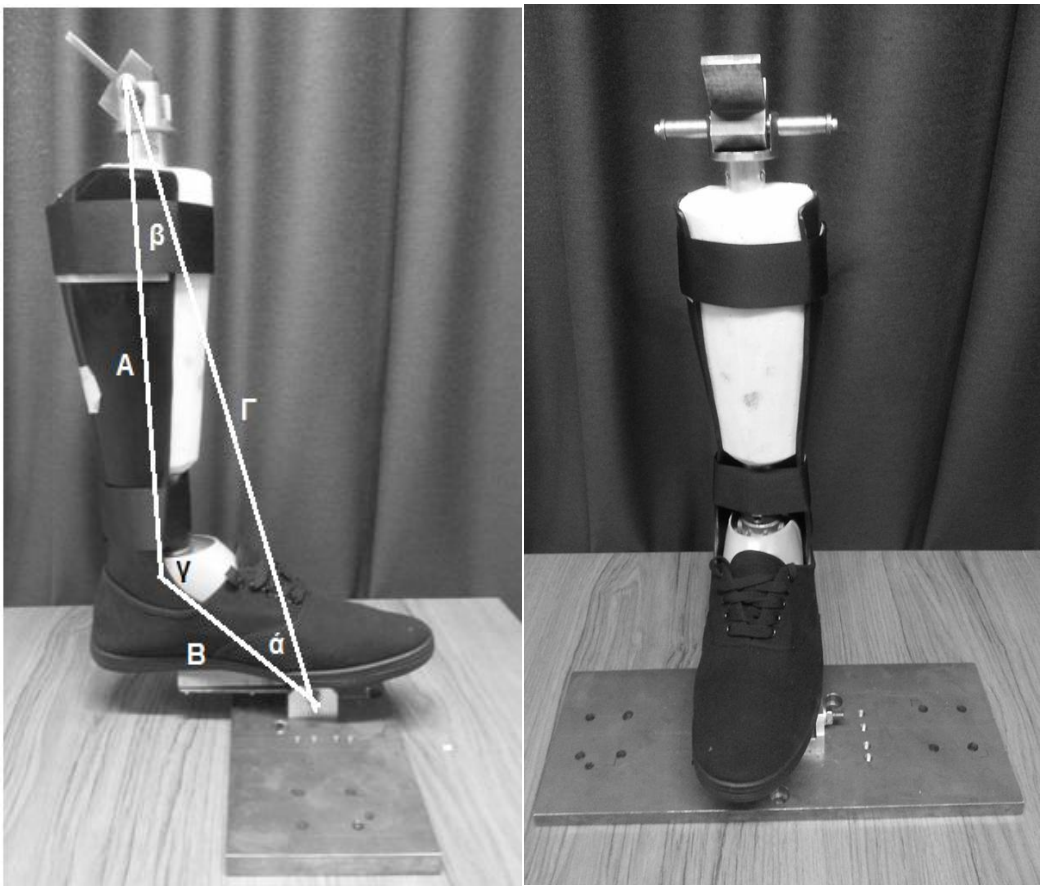

Figure 38 An AFO worn in the effigy leg.

Prior to the test, the metal base was secured in position on the Instron table with three 10mm bolts. The upper crosshead of the material testing machine was lowered at a desired position allowing the lever clamps to grip and secure the upper mounting jig. The solid ankle-foot orthosis was put through five compression cycles. Each cycle was consisted of a load ramp phase lasting for five seconds with a rate of 30N/s. The ramp phase was followed by a position-hold phase lasting for 120 seconds. The two-minute hold phase allowed the operator to use a tape measure to

record the distances α,β,γ as shown in figure 38 entitled “An AFO worn in the effigy leg.”. Those distances were later used to measure the stiffness of the AFO. A typical compression trial as recorded by the Instron Wavematric material testing software (load and crosshead displacement) is shown in figure 39. The maximum load applied on the AFO is equal to 750N; at the end of the last cycle the load drops to zero at a rate of 25N/s. The force and the displacement were recorded at a rate of 10 samples per second. Note that despite the obvious stress relaxation shown in the first diagram, the upper jig’s position was programmed to control the displacement after every ramp phase and thus the experiment is not sensitive to creep.

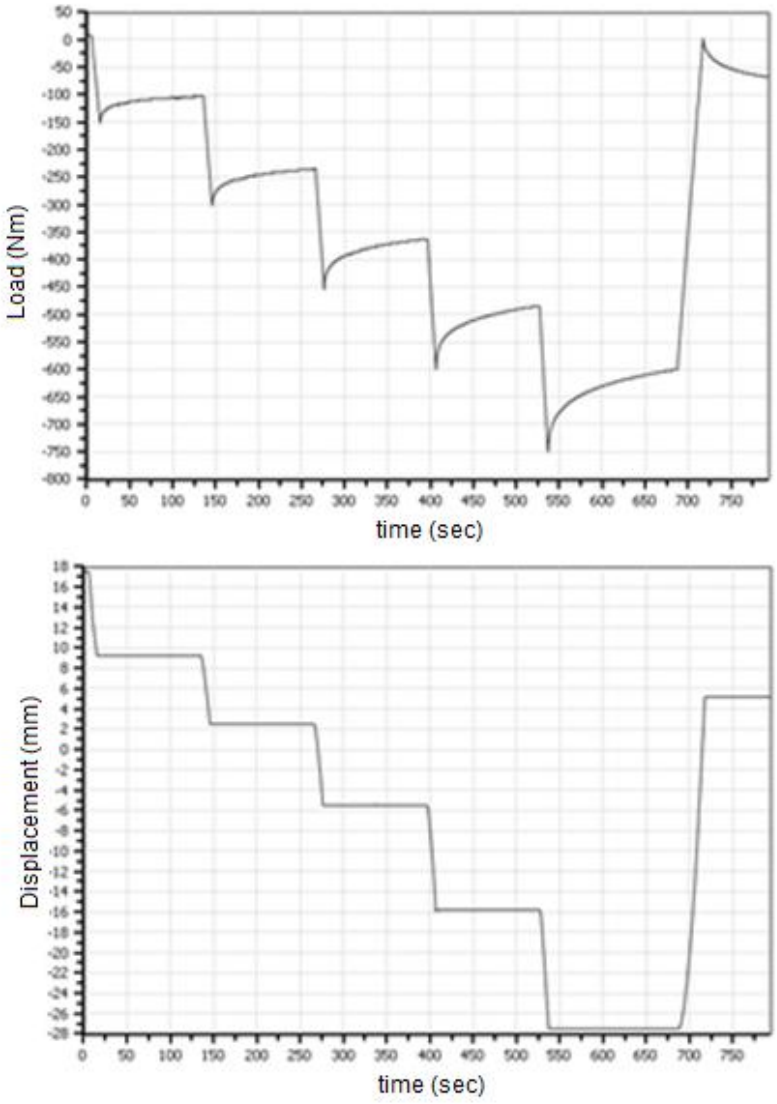

Figure 39 A compression trial as recorded by the Instron Wavematrix material testing software.

Figure 40 shows the fixation of the AFO in the Instron 10000 material testing machine. This particular instant was taken during the compression of the polypropylene AFO during the last compression cycle (notice the buckling of the AFO at the malleoli region).

Figure 40 The AFO/effigy leg assembly in the Instron E10000.

After the completion of the first trial, the AFO was unclamped and allowed to relax for ten minutes. Three compression tests were held in total with the dummy leg worn in the ankle-foot orthosis. Subsequent to the last trial, the effigy leg and the shoe were removed from the assembly and the AFO was clamped once again in the material testing machine. The same procedure was followed again. This time, the loading rate of the AFO was equal to 8/sec instead of 30N/s. The reason for this modification is that during the first set of the compression trials (with the presence of the dummy leg) the AFO was loaded indirectly via the aluminum pipe that represents the tibia. During the second set of trials, the ankle-foot orthosis was loaded directly via a metallic tube penetrating the calf of the orthosis and the likelihood of a permanent deformation in high stresses is highly feasible.

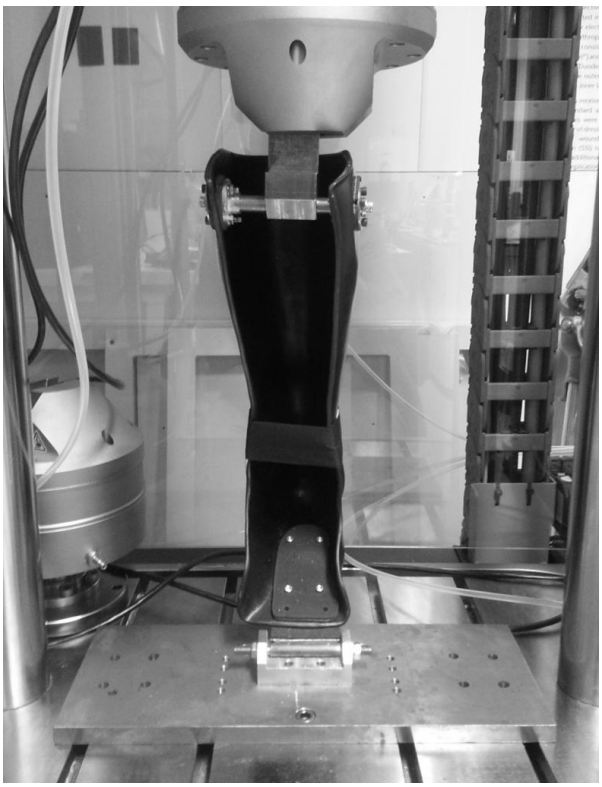

Figure 41 The AFO in the Instron E10000.

3.2 Rigid frame testing procedure

Subsequently, the AFOs were tested with a custom-made device capable of loading the orthosis in the sagittal plane. During the test, the AFO was attached with 3 bolts to the vertical metallic surface of the testing frame. Two different configurations, with the AFO inverted and re-attached to the wall, allowed the application of plantarflexion and dorsiflexion moments. A clock gauge was clamped opposite to the AFO in order to measure the deformation during the loading. Prior to the test, the tip of the gauge was adjusted perpendicular to the posterior part of the orthosis as shown in figure 42. Finally, two holes were drilled in the distal calf region of the AFO; a wire passing through those holes and a weight holder allowed the operator to hang masses and thus, to apply dorsi/plantarflexion moments to the orthosis.

Each AFO was tested twice:

1. With the presence of the effigy leg, while the masses were hanged from the aluminium “tibia” at the level of the knee joint.

2. Without any leg/shoe, while the masses were hanged from the holes drilled in the calf region of the AFO.

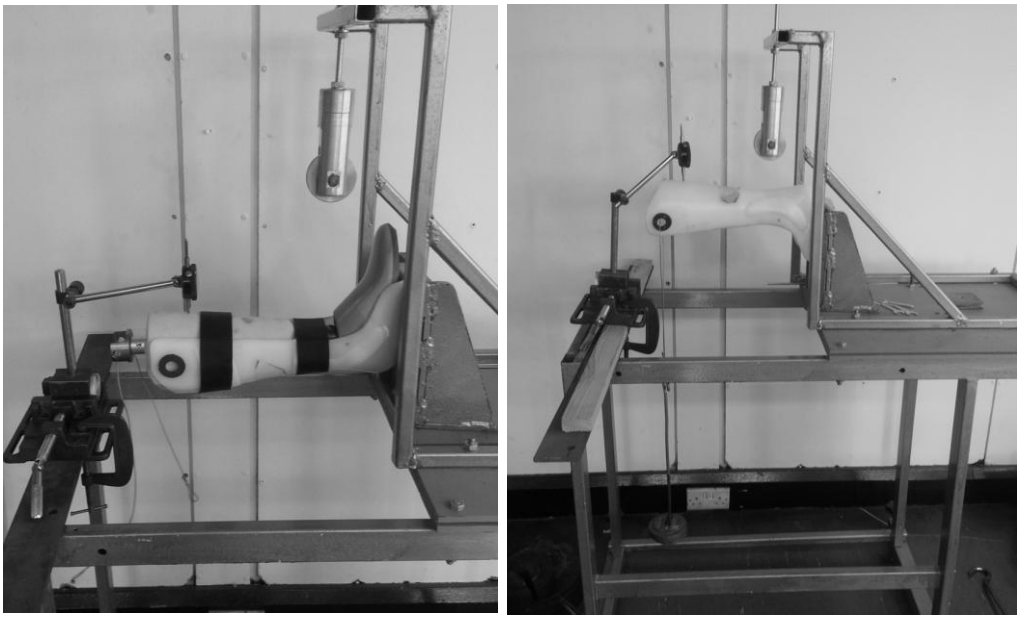

Figure 42 From left to right: Dorsiflxion test of a 4.6 co-polymer AFO with the presence of the effigy leg and a plantarflexion test without the leg.

During the test, masses were gradually added onto the weight holder (one kilogram at a time, with a maximum of eight kilograms). Immediately after the application of the load, the displacement was recorded. It should be noted that this method is sensitive to creep.

3.3 Data processing-Instron 10000

For the calculation of the stiffness of the ankle-foot orthosis, the moment about the center of the axis passing through the maleolli and the deformation angle of the AFO (angle γ as shown in figure 43) are needed. The moment about the malleolli can be calculated if the load given by the Instron Wavematric material testing software is multiplied with the moment arm:

$$M(ankle) = F * A * \sin(\beta)$$

The angle γ and thus, the deformation angle of the AFO can be calculated via the following equation:

$$\gamma\ (rad) = cos^{-1}[\frac{A^2 + B^2 - \Gamma^2}{2 * A * B}]$$

Where,

A=distance from the ankle axis to the upper fixation point,

B=distance from the ankle axis to the lower fixation point,

Γ=distance between the two fixation points.

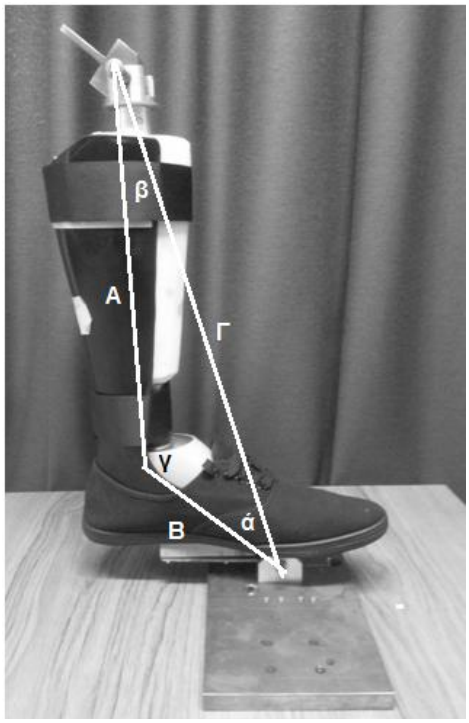

Figure 43 Dimensions for the calculation of the stiffness.

The distance Γ can be found based on the displacement and the location of the upper jig as given by the Instron Wavematrix softwarre. For the calculation of the two other distances, A and B, two different approaches were followed:

1. Distances A and B are constants and equal to 345 and 185 mm respectively (as measured prior to the test). This approach was followed by Major et al. (2004) and Hagenbeek (2013).

2. Distances A and B are variables, changing throughout the compression test due to the elastic deformation of the AFO and they are measured with a ruler during the displacement-hold phase of the test. This approach was never implemented in the literature and it is believed to be a more accurate method to measure the flexibility of an ankle-foot orthosis.

3.4 Data processing-Rigid metal frame

The processing of the data acquired from the metal frame testing was similar to the one followed with the instron data processing. Prior to the test, the AFOs were once again marked in the maleoli prominences. Following every masses increment, the load from the hanging weights and the displacement, as shown in the clock gauge (in inches), was recorded.

Finally, the data were transferred in an Excel spreadsheet. The displacement was converted in mm and the same functions as the one used in the Instron-Data processing were implemented.

4 Results

A 4.6 mm black co-polymer solid AFO was tested in the Instron E10000 with/without the presence of the effigy leg. The data gathered were analysed in two different approaches: (1) the distance between the lower jig and the medial malleolus prominence of the AFO and the distance connecting the medial malleolus and the upper jig were considered constants and equal to 345 and 185 mm respectively and (2) those distances were variables changing throughout the compression test due to the elastic deformation of the AFO.

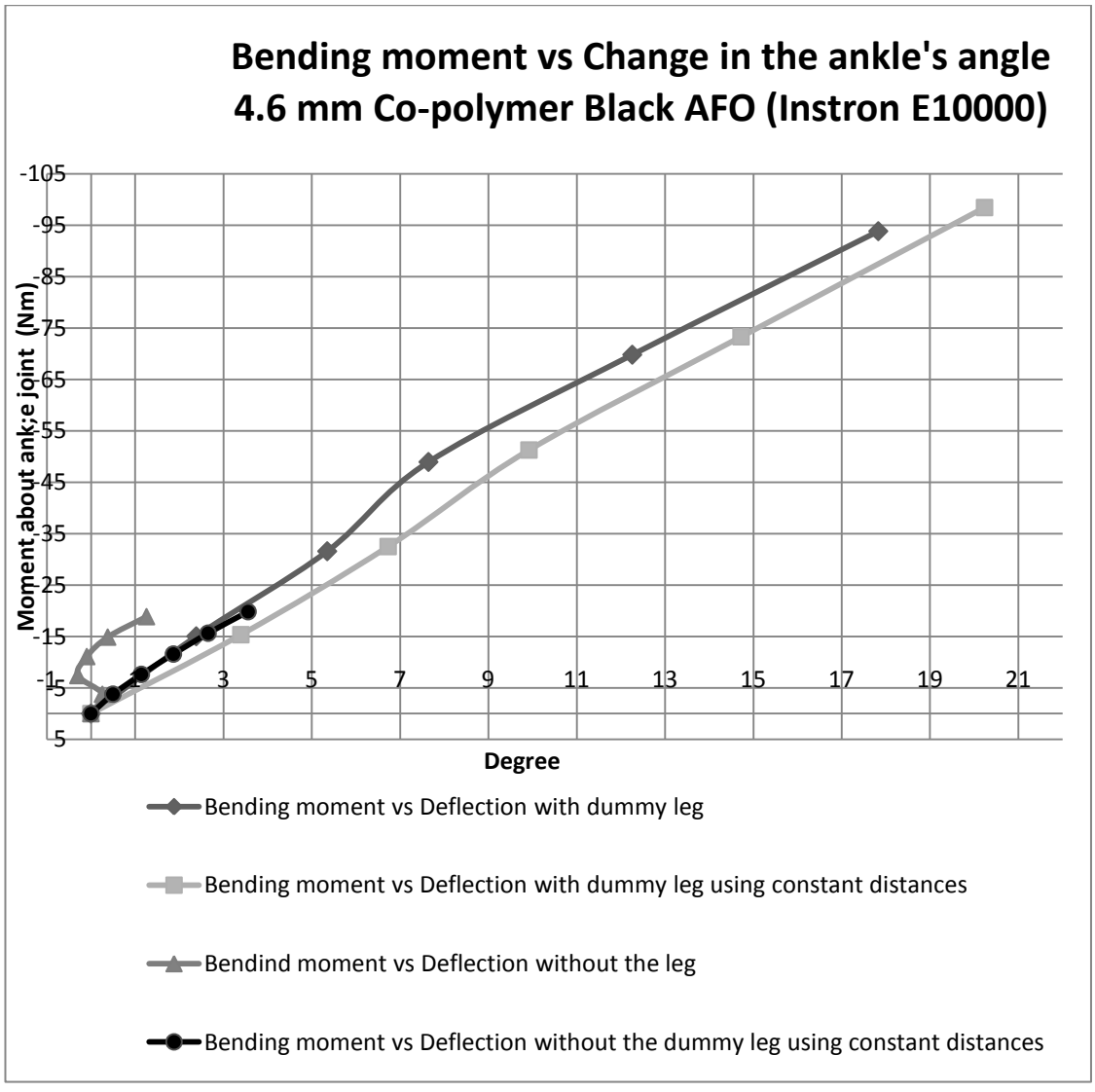

Figure 44 Bending moment vs Deflection angle (Instron E1000).

Figure 44 shows only the bending stiffness (dorsiflexion) of the 4.6 mm black co-polymer AFO. It should be noted that each stiffness curve is the product of three individual tests (the mean value). No data were gathered during the tension test (plantarflexion). The reason of this omission was the sudden termination of the plantarflexion test in every trial with the presence of the effigy leg. It was noted that between 250-350N (e.g. 24-34 Nm) the material testing machine would suddenly stop operating. It appears that the reason for this discontinuation was that the effigy leg would violently sleep out of the ankle-foot orthosis causing the program to suddenly terminate due to standard safety displacement limits. A steeper curve in the bending moment/degree diagram indicates a stiffer ankle-foot orthosis. As expected, when an artificial limb is introduced in the orthosis the assembly is less flexible.

Figure 45 demonstrates the Stiffness of the 4.6 co-polymer AFO with carbon fibre corrugations as measured with the custom-made device. Both the stiffness of the AFO solely and the stiffness of the AFO/leg assembly are presented. In both curves the hysteresis loops due to the viscoelastic properties of the polymer are obvious. As expected, when an effigy leg is introduced in the AFO, the assembly is stiffer; this can be better seen in the positive quadrant which represents the plantarflexion motion. On the other hand, during dorsiflexion (i.e. in the negative quadrant), the stiffness in both cases seems to be in good agreement. The reader should notice that since the masses were hanged more proximally in the case of the AFO/leg assembly (figure 42), the moment arm was larger and thus, the moment applied in the ankle joint was greater as well. Because of that, the curves representing the stiffness of the AFO/leg assembly will reach higher moment values. Another thing to notice is that the mass of the effigy leg distal of the ankle joint, which was equal to 1.5 kg (the mass of the leg was 1.65kg minus the mass of the single-axis foot), was included in the calculations; nevertheless, the moment due to the mass of the effigy les was, in any instance, less than 0.25 Nm. Figure 46 demonstrates the relevant curves for the 6mm homo-polymer AFO. In this case, the two stiffness loops are in a very good agreement.

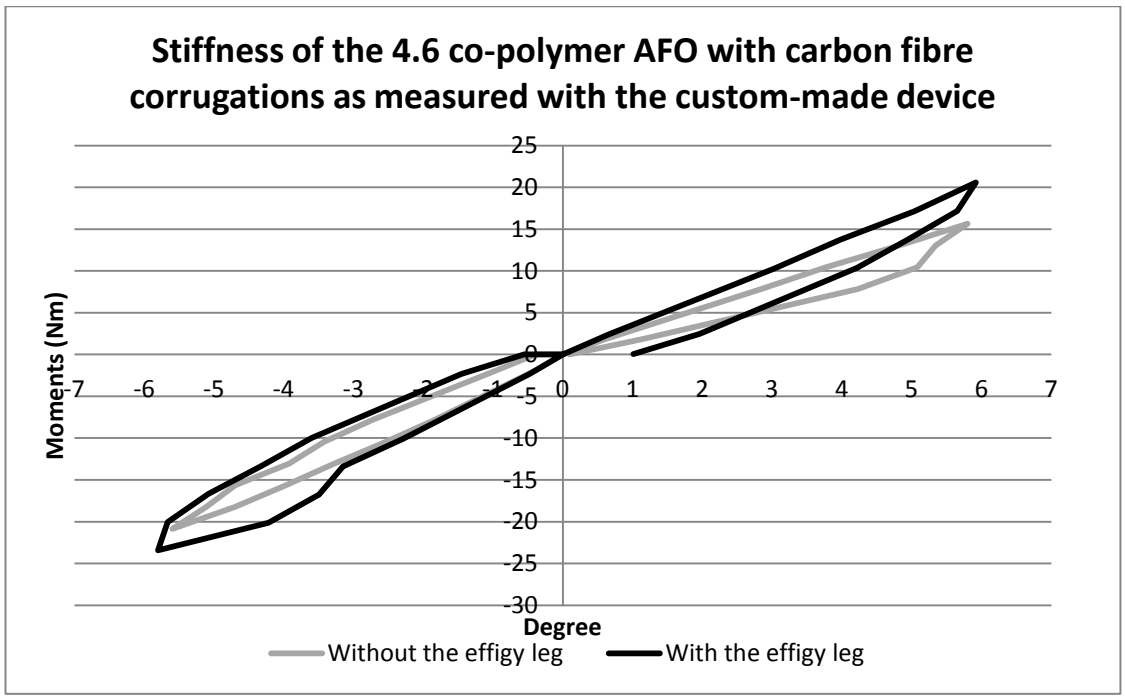

45

Figure 45 Stiffness of the 4.6 co-polymer AFO with carbon fibre corrugations as measured with the custom-made device.

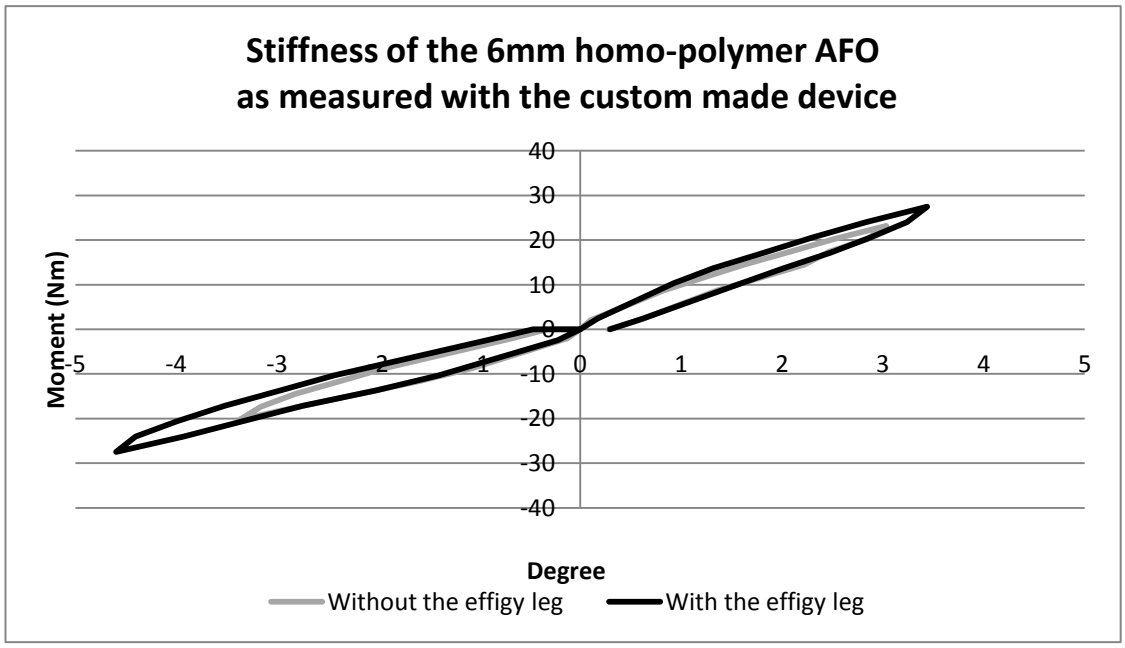

Figure 46 Stiffness of the 6mm homo-polymer AFO as measured with the custom made device.

[4] Moment refers to the moment around the ankle joint
[5] Degree refers to the degree of flexion

Figure 47 and Figure 48 illustrate the stiffness of the 4.6 co-polymer AFO and the stiffness of the 6mm homo-polymer AFO, without the leg, as measured with both devices respectively. In both cases, the stiffness of the same ankle-foot orthosis is underestimated when measured with the custom-made device. According to the author's viewpoint, this inconsistency is due to the creep of the orthosis when loaded in the custom made device; it was observed, immediately after hanging the masses, that the AFO will continue to deform under the influence of the constant load and the displacement as recorded by the clock gauge will steadily rise. On the other hand, during the loading in the Instron E10000, the hold-displacement phase of the moving Instron's head will not allow the AFO to creep.

As mentioned earlier in the methodology, during the measurement with the custom-made device, the operator recorded the displacement *immediately* after the application of the load. Nevertheless, errors due to the cold flow of the polypropylene are expected and thus, the stiffness of the AFO when measured in the custom made device should be undervalued.

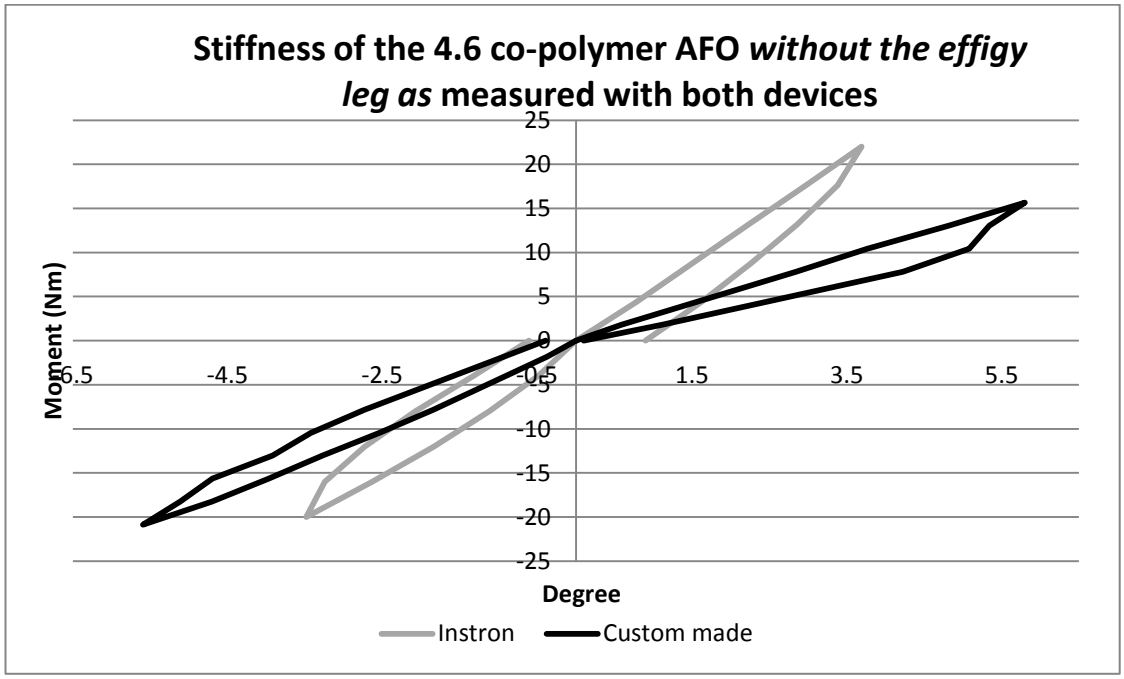

Figure 47 Stiffness of the 4.6 co-polymer AFO with carbon fibre Corrugations without the effigy leg as measured with both devices.

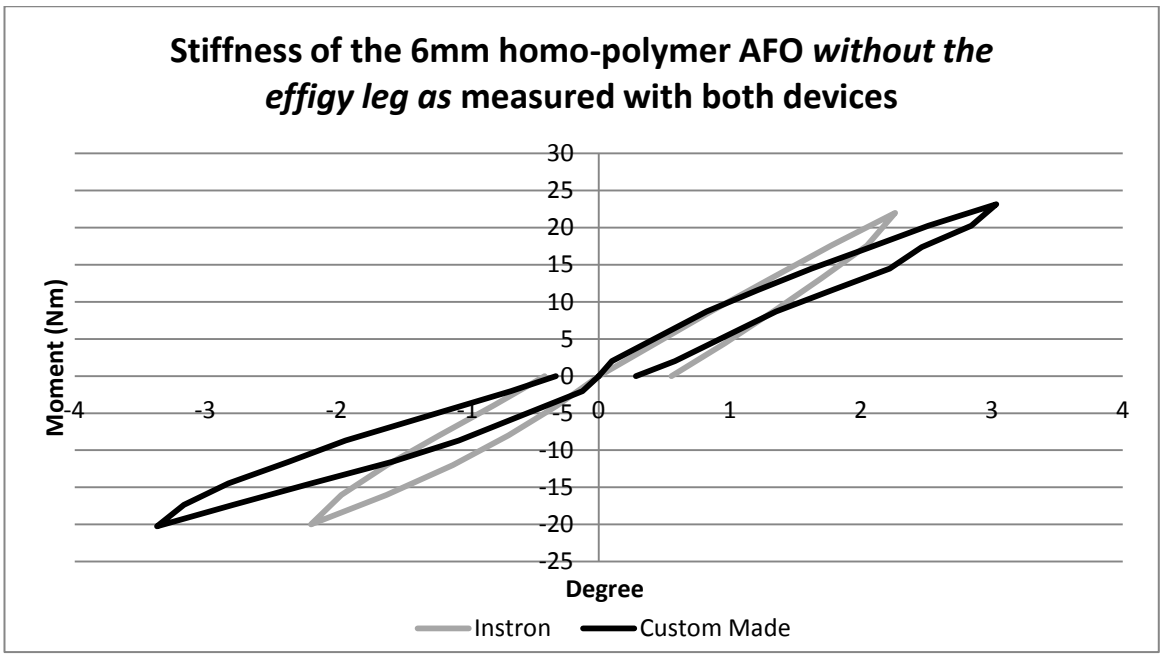

[6]

Figure 48 Stiffness of the 6mm homo-polymer AFO without the effigy leg as measured with both devices.

Figure 49 and figure 50 illustrate the corresponding stiffness curves for the two different types of AFO. However, this time the effigy leg is included in the trial. For the aforementioned reasons, when the AFO is measured in the custom-made device, it is found to be more flexible.

Figure 51 points up the stiffness of the 4.6mm AFO, with and without the presence of the effigy leg, as measured in the Instron E10000. The equivalent graph for the 6mm orthosis is presented in figure 52. As explained before concerning figures 45 and 46, when an effigy leg is introduced in the AFO, the assembly is stiffer.

Finally, the last two graphs of this chapter, figure 53 and 54, demonstrate the obvious, i.e., that the thicker 6mm ankle-foot orthosis is stiffer than the 4.6mm.

[6] The custom Made refers to the custom-made rig

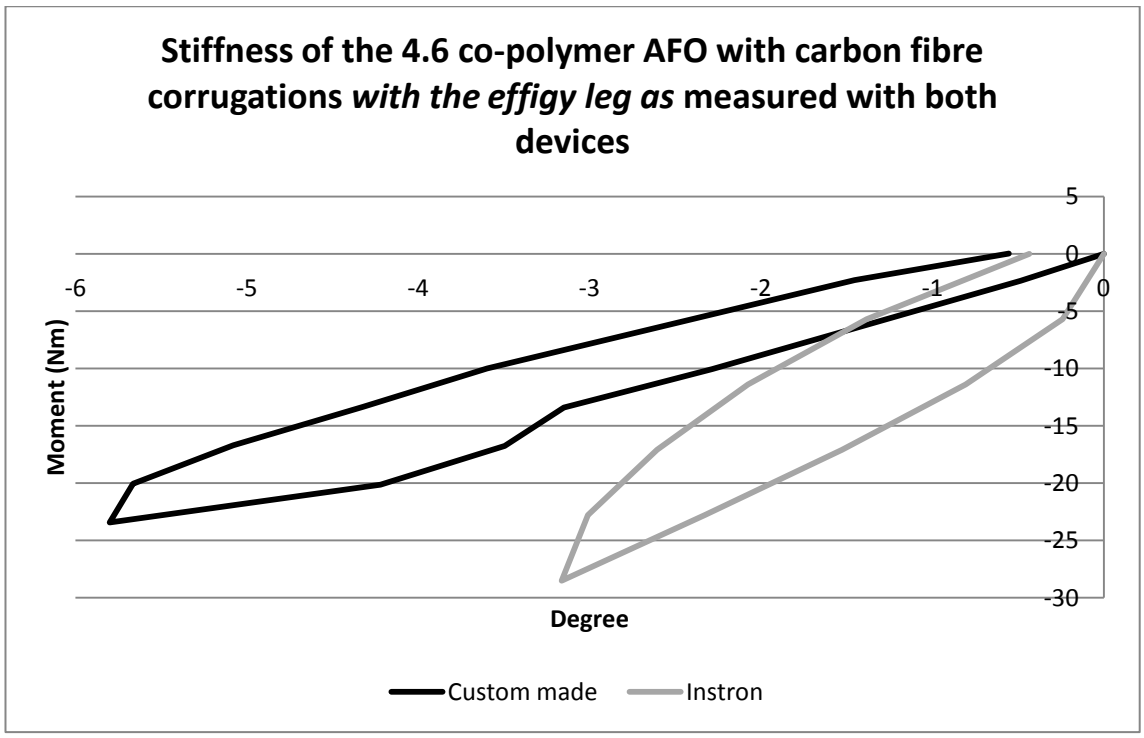

Figure 49 Stiffness of the 4.6 co-polymer AFO with carbon fibre Corrugations with the effigy leg as measured with both devices.

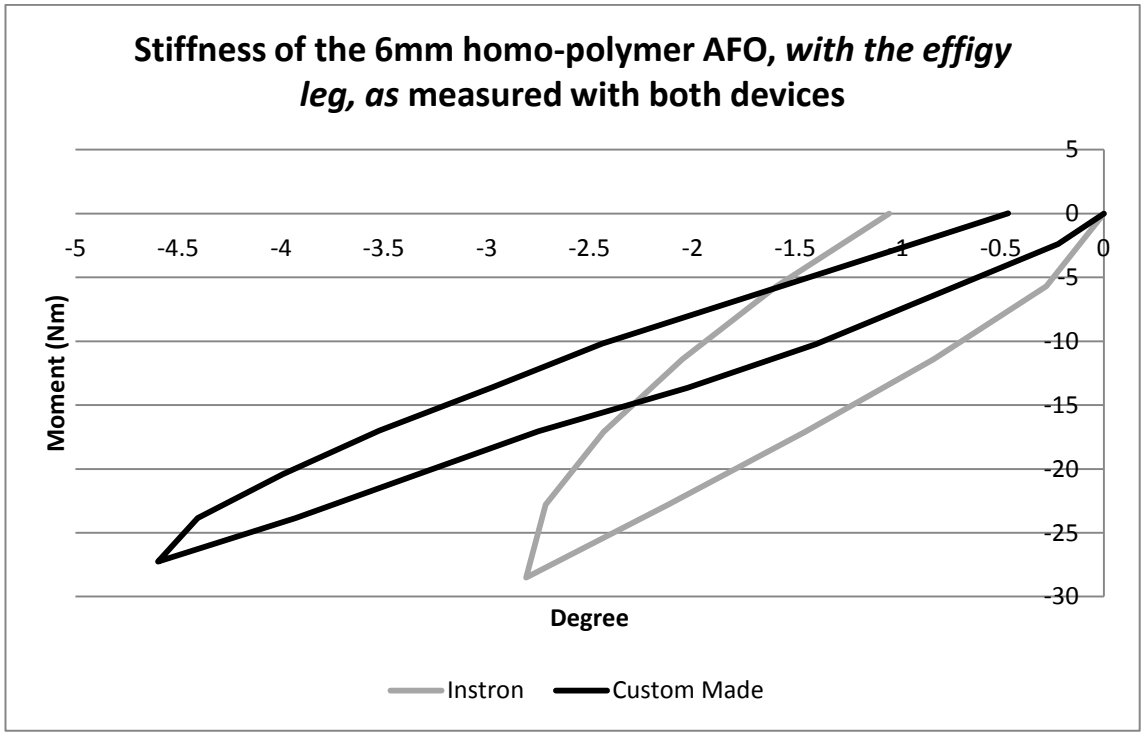

Figure 50 Stiffness of the 6mm homo-polymer AFO, with the effigy leg, as measured with both devices.

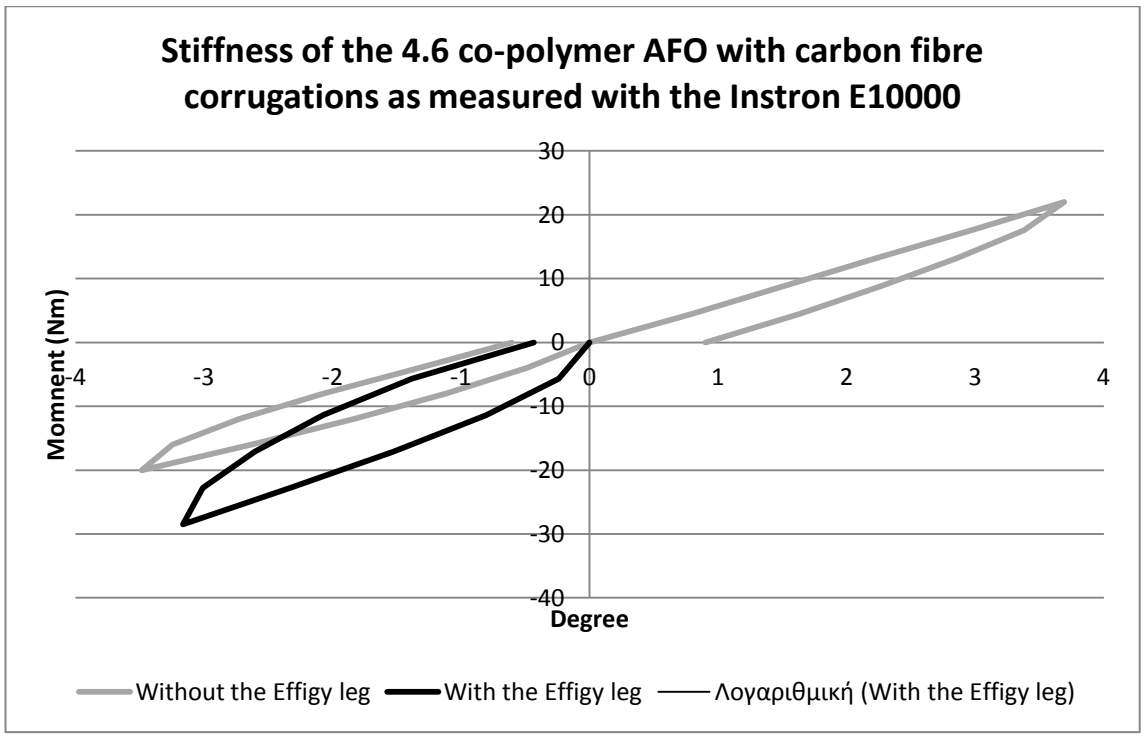

Figure 51 Stiffness of the 4.6 co-polymer AFO with carbon fibre Corrugations as measured with the Instron E10000.

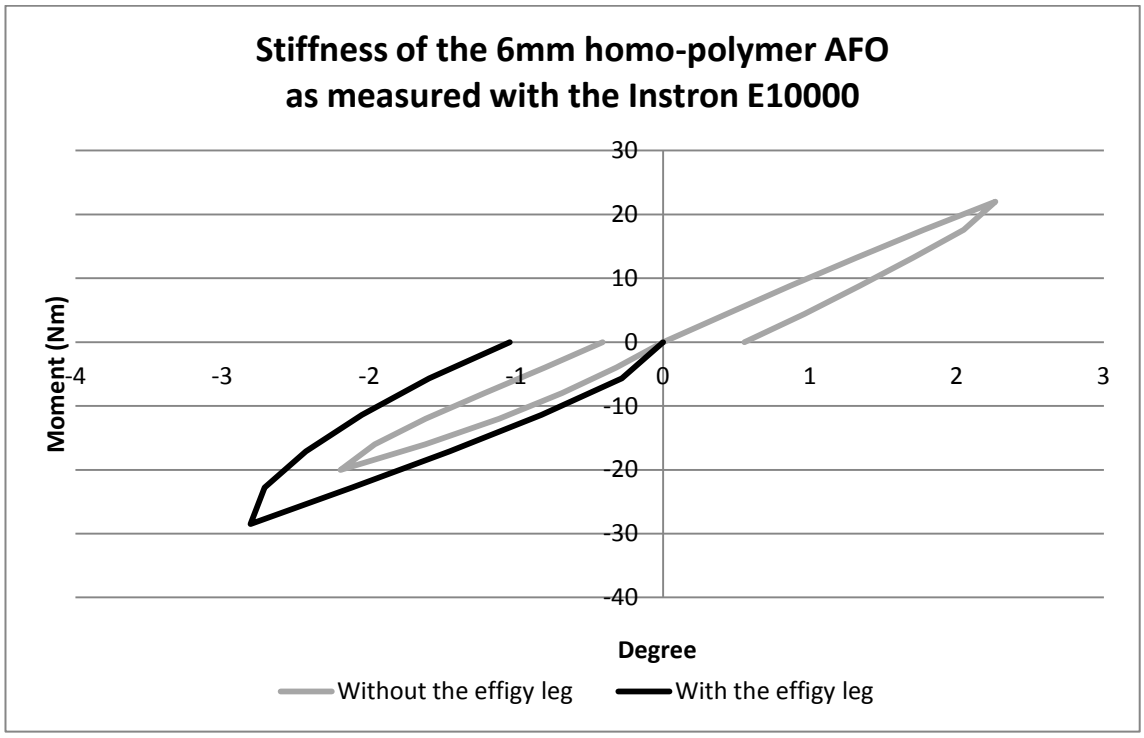

Figure 52 Stiffness of the 6mm homo-polymer AFO as measured with the Instron E10000.

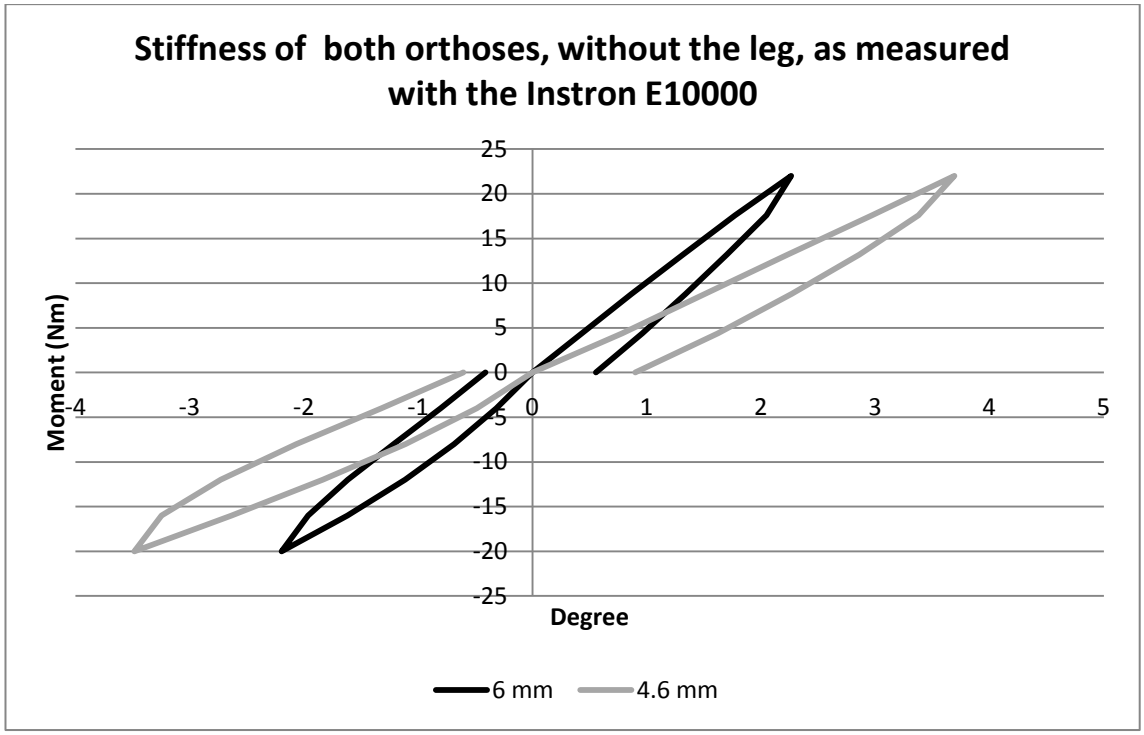

Figure 53 Stiffness of both orthoses, without the leg, as measured with the Instron E10000.

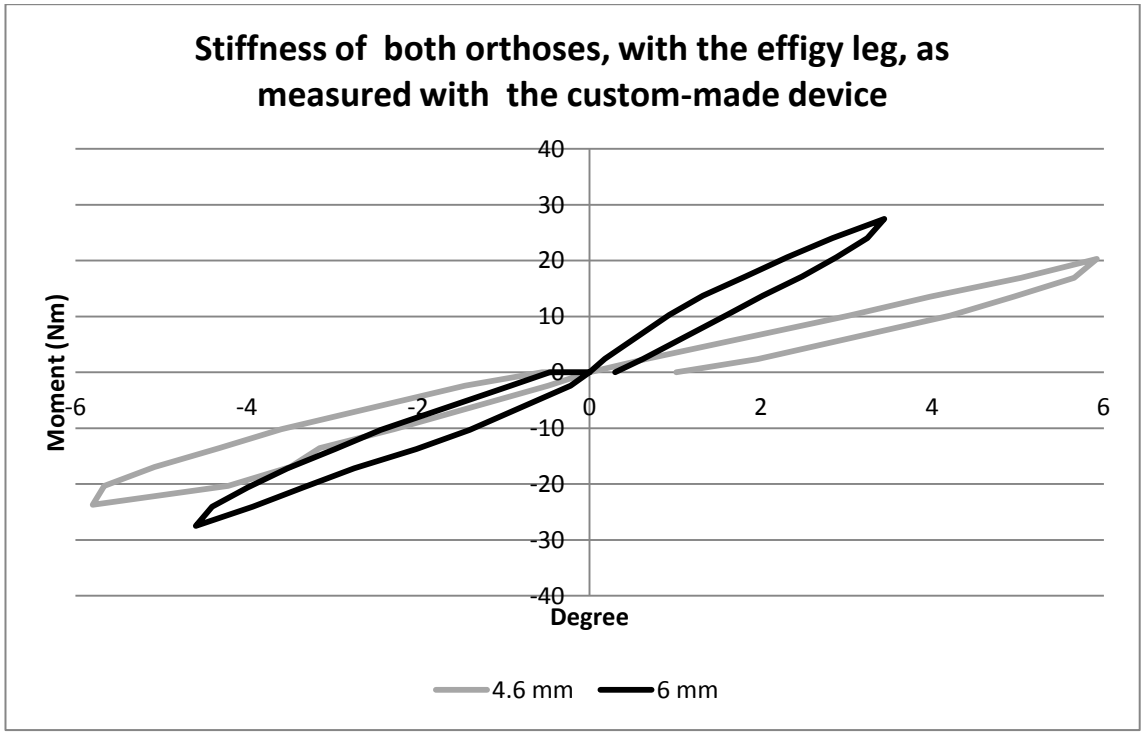

Figure 54 Stiffness of both orthoses, with the effigy leg, as measured with the custom-made device.

5 Discussion

In section 2.3 entitled “Bench testing methods for determining stiffness of ankle-foot orthosis”, eight different methods for determining the stiffness of an AFO are critically described. In the aforementioned section, devices with different degrees of sophistication were reviewed. According to the author's perspective, twelve different parameters were considered during the investigation and the evaluation of those bench testing methods. Those criteria are listed in section 2.2.1.1 entitled as “bench testing analysis”.

It is the author’s belief that the most suitable method for determining the stiffness of an ankle-foot orthosis is presented by Sumiya et al. (1996). This particular model is cost effective, easy to build and with high reproducibility. More important, Sumiya’s model enables the load to be applied always vertical to the AFO. That way, the AFO’s sole is not compressed during the test and the experimenter can easily and accurate measure the moments applied in the ankle joint at all times.

Bregman et al. (2009) also designed an excellent device able to measure the stiffness of the AFO at the ankle joint and the metatarsal-phalangeal joint. What is more, this study describes the only test that the AFO was tested in combination with a shoe. Finally, this is the first study that portrays the flexibility of the AFO in combination with AFO neutral angles (casting angle).

Cappa et al. (2003) and Klasson et al (1998) developed testing apparatus capable of evaluating the stiffness of an orthosis in more than one planes. Those studies describe the only two devices in literature able to perform this type of measurement. However, both approaches have increased design and set-up complexity, while the testing procedure is challenging and time consuming.

Among those eight bench testing approaches, two of them were implemented in this study: the mechanical testing by Major et al. (2004) described in section 2.3.1

and the bending test by Ross et al. (1999) (and Hagenbeek,2013) described in section 2.3.3.. Those two methods were not followed blindly; firstly, the implication of using an effigy leg during the testing procedure was investigated. Several authors published articles describing bench testing methods that include a surrogate limb (Bregman et al., 2009; Cappa et al., 2003; Klasson et al., 1998). Nevertheless, there is no evidence in the literature that the presence of an effigy leg can significantly alter the stiffness of an AFO. Enlightening stiffness diagrams, relating the presence of a dummy leg to the flexibility of an AFO, are presented in chapter 4 and discussed later on in this chapter.

Secondly, it is the author's opinion, that the mathematical data processing of the Instron testing existing in the literature is imprecise. As a result, the data gathered from the tests were analysed in two different approaches. The results obtained from this analysis are presented later on in this chapter.

Thirdly, the two abovementioned methods for determining the AFO stiffness represent the two "edges" of the existing literature: Major's method is utilizing a material testing machine (Instron 1185), which is an extremely costly but also exceptionally accurate machinery; on the other hand, Ross et al., had used only hanging masses and a dial gauge to perform the same measurement. Thus, the question posed is whether the selection of the machinery can *significantly* alter the results obtained.

5.1 The implication of using an effigy leg during the testing procedure

In order to quantify the influence that the effigy leg has on the stiffness of the ankle-foot orthosis, the data of the 4.6mm co-polymer AFO testing in the Instron E10000 were further processed. In more detail, the stiffness curves during the loading and unloading of the AFO were estimated; the four third-degree polynomial equations and their correlation coefficient are presented below (as indicated in figure 55).

- $y = 0.8909x^3 + 4.4481x^2 + 11.999x + 5.9082$, $R^2 = 0.9974$
- $y = 0.1788x^3 + 1.4519x^2 + 8.6306x$, $R^2 = 0.9999$
- $y = 1.6339x^3 + 6.082x^2 + 13.089x + 4.7338$, $R^2 = 0.9945$
- $y = 1.1329x^3 + 6.8384x^2 + 19.348x$, $R^2 = 0.9952$

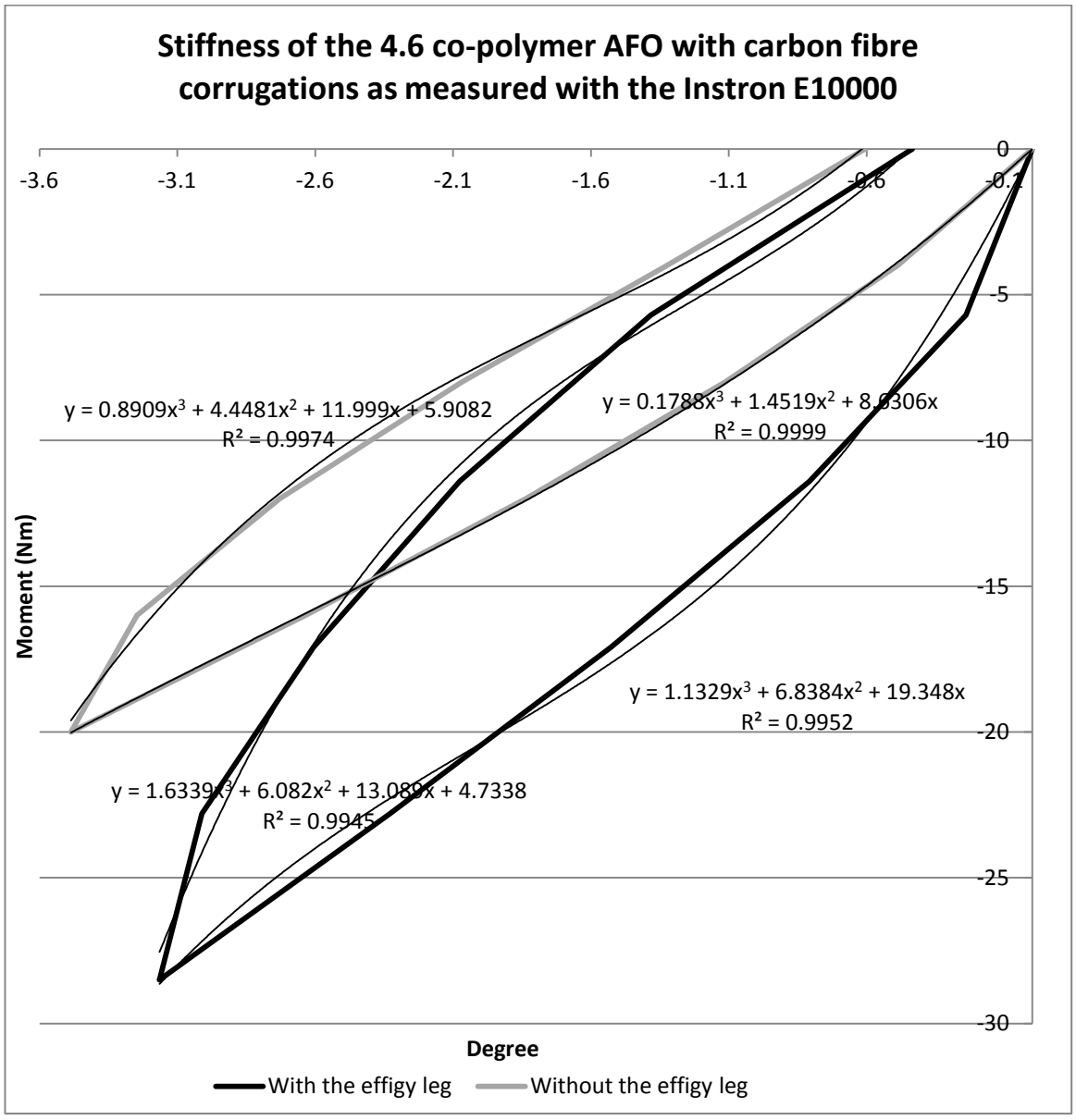

Figure 55 Stiffness of the 4.6 co-polymer AFO with carbon fibre Corrugations as measured with the Instron E10000 (ii)

Based on these four equations, the stiffness of the AFO, with and without the effigy leg, was calculated throughout the whole range of motion (from 0° to -3.3°, with 0.1° increments). For the reader's convenience, in these equations, x stands for the degree of deformation of the AFO in the ankle joint, y stands for the moment applied in the AFO while the stiffness is defined as moment per degree of deformation.

Table 1 Degree of deformation and moments applied in the 4.6mm co-polymer AFO

Path:	**Unloading path, without the leg**	**Loading path, without the leg**	**Unloading path, with the leg**	**Loading path, with the leg**
Equation:	*y=0.8909x3 + 4.4481x2 + 11.999x + 5.9082*	*y = 0.1788x3 + 1.4519x2 + 8.6306x*	*y = 1.6339x3 + 6.082x2 + 13.089x + 4.7338*	*y = 1.1329x3 + 6.8384x2 + 19.348x*
Degree	**Moment (Nm)**	**Moment (Nm)**	**Moment (Nm)**	**Moment (Nm)**
-0.1	4.75	-0.85	3.48	-1.87
-0.2	3.68	-1.67	2.35	-3.61
-0.3	2.68	-2.46	1.31	-5.22
-0.4	1.76	-3.23	0.37	-6.72
-0.5	0.91	-3.97	-0.49	-8.11
-0.6	0.12	-4.69	-1.28	-9.39
-0.7	-0.62	-5.39	-2.01	-10.58
-0.8	-1.30	-6.07	-2.68	-11.68
-0.9	-1.94	-6.72	-3.31	-12.70
-1	-2.53	-7.36	-3.91	-13.64
-1.1	-3.09	-7.97	-4.48	-14.52
-1.2	-3.62	-8.57	-5.04	-15.33
-1.3	-4.13	-9.16	-5.59	-16.08
-1.4	-4.62	-9.73	-6.15	-16.79
-1.5	-5.09	-10.28	-6.73	-17.46
-1.6	-5.55	-10.82	-7.33	-18.09
-1.7	-6.01	-11.35	-7.97	-18.69
-1.8	-6.47	-11.87	-8.65	-19.28
-1.9	-6.94	-12.38	-9.39	-19.85
-2	-7.42	-12.88	-10.19	-20.41
-2.1	-7.92	-13.38	-11.06	-20.97
-2.2	-8.45	-13.86	-12.02	-21.53
-2.3	-9.00	-14.35	-13.08	-22.11
-2.4	-9.58	-14.82	-14.23	-22.71
-2.5	-10.21	-15.30	-15.51	-23.33
-2.6	-10.88	-15.77	-16.90	-23.99

-2.7	-11.60	-16.24	-18.43	-24.69
-2.8	-12.37	-16.71	-20.10	-25.43
-2.9	-13.21	-17.18	-21.92	-26.23
-3	-14.11	-17.65	-23.91	-27.09
-3.1	-15.08	-18.13	-26.07	-28.01
-3.2	-16.13	-18.61	-28.41	-29.01
-3.3	-17.26	-19.10	-30.94	-30.09

Table 2 Stiffness of the 4.6mm AFO

Path:	**Unloading path, without the leg**	**Loading path, without the leg**	**Unloading path, with the leg**	**Loading path, with the leg**
Equation:	y=0.8909x3 + 4.4481x2 + 11.999x + 5.9082	y = 0.1788x3 + 1.4519x2 + 8.6306x	y = 1.6339x3 + 6.082x2 + 13.089x + 4.7338	y = 1.1329x3 + 6.8384x2 + 19.348x
Degree	**Stiffness (Nm/Degree)**	**Stiffness (Nm/Degree)**	**Stiffness (Nm/Degree)**	**Stiffness (Nm/Degree)**
-0.1	-47.52[7]	8.49	-34.84	18.68
-0.2	-18.40	8.35	-11.73	18.03
-0.3	-8.95	8.21	-4.37	17.40
-0.4	-4.41	8.08	-0.92	16.79
-0.5	-1.82	7.95	0.99	16.21
-0.6	-0.20	7.82	2.14	15.65
-0.7	0.88	7.70	2.87	15.12
-0.8	1.63	7.58	3.35	14.60
-0.9	2.15	7.47	3.68	14.11
-1	2.53	7.36	3.91	13.64
-1.1	2.81	7.25	4.07	13.20
-1.2	3.02	7.15	4.20	12.77
-1.3	3.18	7.05	4.30	12.37
-1.4	3.30	6.95	4.40	11.99
-1.5	3.39	6.86	4.49	11.64
-1.6	3.47	6.77	4.58	11.31
-1.7	3.54	6.68	4.69	11.00
-1.8	3.60	6.60	4.81	10.71
-1.9	3.65	6.52	4.94	10.44
-2	3.71	6.44	5.09	10.20
-2.1	3.77	6.37	5.27	9.98
-2.2	3.84	6.30	5.46	9.79
-2.3	3.91	6.24	5.69	9.61
-2.4	3.99	6.18	5.93	9.46

[7] Values in dark gray fond were considered as outliers.

-2.5	4.08	6.12	6.20	9.33
-2.6	4.18	6.06	6.50	9.23
-2.7	4.30	6.01	6.83	9.14
-2.8	4.42	5.97	7.18	9.08
-2.9	4.55	5.92	7.56	9.04
-3	4.70	5.88	7.97	9.03
-3.1	4.87	5.85	8.41	9.04
-3.2	5.04	5.82	8.88	9.07
Mean stiffness	***2.571***	***6.875***	***4.636***	***12.114***

Subsequently, the differences in stiffness between the two cases (with and without the effigy leg), for both the loading and the unloading path, were found. Finally, the mean value and the standard deviation of this difference were calculated. The mean value for the unloading path was found equal to 2.1314 Nm/degree with a standard deviation of 1.01 Nm/degree, whereas the mean value for the loading path was equal to 5.182 Nm/degree with a standard deviation of 2.21 Nm/degree. According to the author's personal opinion, this difference in stiffness is considered noteworthy and the results obtained from a study that uses an effigy leg should not be related with a study that does not. Furthermore, it is the author's opinion that the effigy leg supports the soft parts of the AFO (e.g. the sole) from bending abnormally during the bench test, enables the experimenter to mimic the loading of the AFO during normal ambulation, whereas the leg's ankle joint allows the AFO to freely deform in the malleoli region under the influence of the applied moment. For all those reasons, it is concluded, that an effigy leg should be used during the bench stiffness testing.

5.2 Mathematical data processing

Regarding the stiffness testing implemented in this study, a 4.6 mm black co-polymer solid AFO was tested in the Instron E10000 with and without the presence of the effigy leg. The data presented in figure 44, were analysed, as mentioned before, in two different approaches:

1. The distance between the lower jig and the medial malleolus prominence of the AFO and the distance connecting the medial malleolus and the upper jig were considered constants and equal to 345 and 185 mm respectively. This approach was followed in the literature by Major et al. (2004) and Hagenbeek (2013).

2. Those distances were variables changing throughout the compression test due to the elastic deformation of the AFO and they are measured during the displacement-hold phase of the test. This approach was never implemented in the literature before.

The results of this study are unambiguous: the bending moment vs deflection angle line corresponds to a second-degree polynomial equation. This finding is confirmed by the high correlation coefficient (0.9984 and 0.9987). Furthermore, between the two approaches, there is an error with a mean value equal to 0.8814 Nm/degree and a standard deviation of 0.42595 Nm/degree. Thus, according to the author's point of view, this difference cannot be considered as negligible and the data processing implemented in this study is considered more accurate than the one followed in the literature.

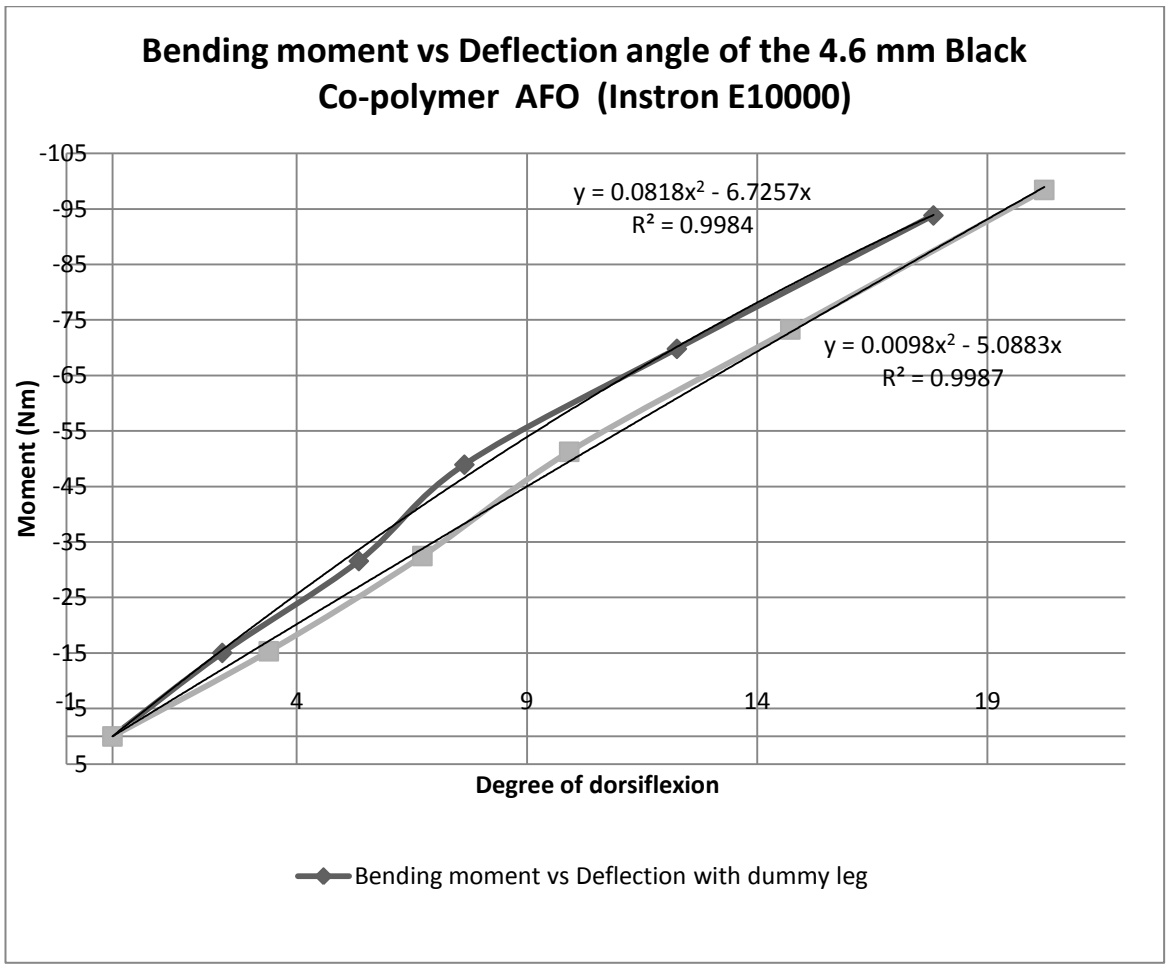

Figure 56 Bending moment vs Deflection angle of the 4.6 mm Black AFO (ii)

5.3 The selection of the machinery

Finally, in order to answer the last posed question, whether the selection of the machinery can *significantly* alter the results, the data obtained from the two different devices were processed in a similar manner. The four polynomial equations and their correlation coefficient are presented below. Figure 57 display graphically those four equations. Once again, the moment applied in the malleoli region(y) was calculated via those four equations (table 3). Finally, the stiffness of the 4.6mm AFO, from 0° to 3.6° of dorsiflexion, as measured in the Instron and the custom-made machine are shown in table 4.

- $y = -0.235x^2 + 2.538x + 0.8898$, $R^2 = 0.9986$

- $y = 0.8909x^3 + 4.4481x^2 + 11.999x + 5.9082$, $R^2 = 0.9974$
- $y = 0.1178x^2 + 4.3852x - 0.0954$, $R^2 = 0.9998$
- $y = 0.5064x^2 + 7.3968x - 0.2383$, $R^2 = 0.9992$

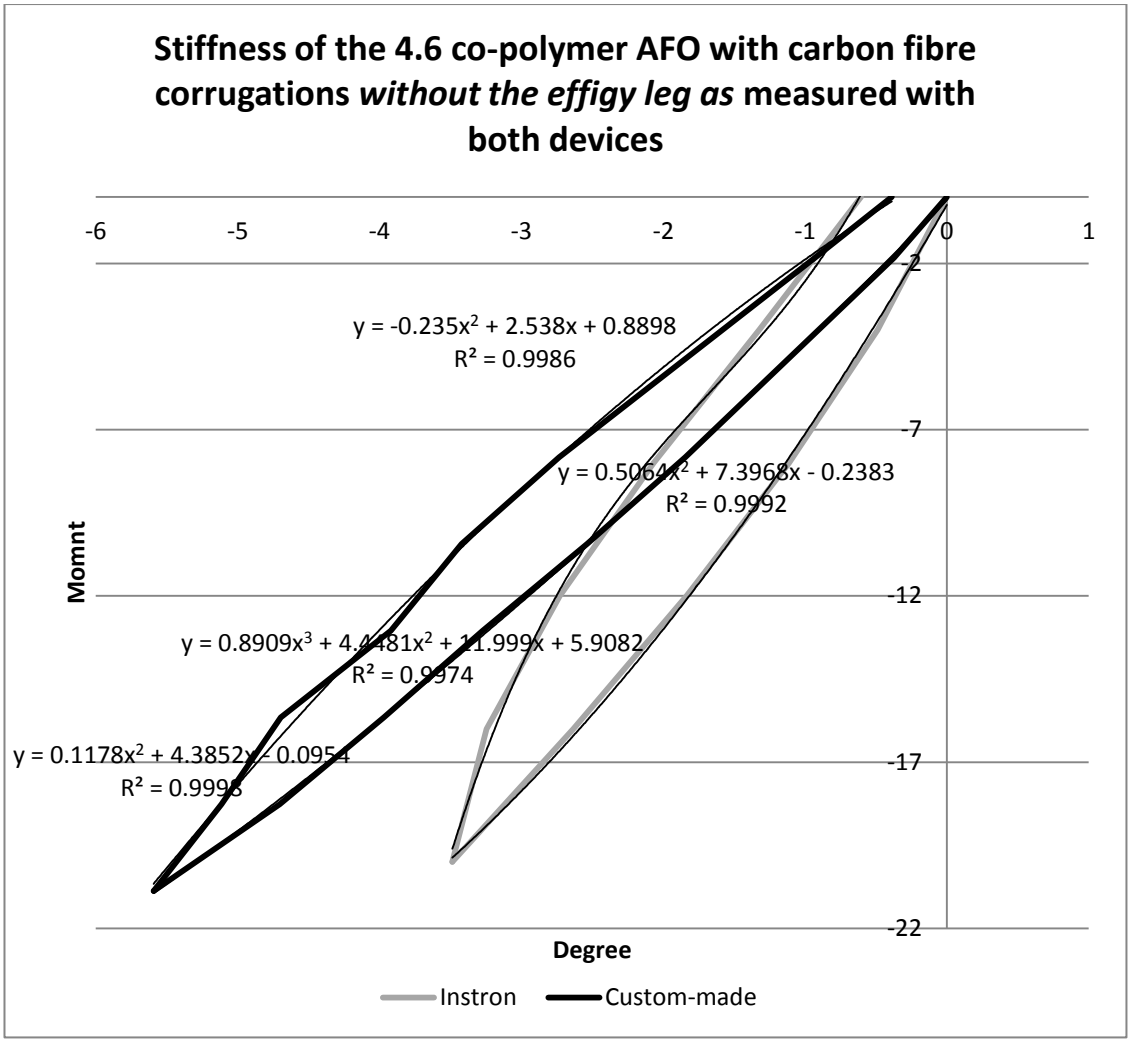

Figure 57 Stiffness of the 4.6 co-polymer AFO with carbon fibre Corrugations without the effigy leg as measured with both devices (ii)

Table 3 Degree of deformation and moments applied in the 4.6mm AFO as measured with both devices

Path:	Unloading in the custom-made	Loading in the custom-made	Unloading in the Instron	Loading in the Instron
Equation:	y= -0.235x2 + 2.538x + 0.8898	y=0.1178x2 + 4.3852x - 0.0954	y = 0.8909x3 + 4.4481x2 + 11.999x + 5.9082	y = 0.5064x2 + 7.3968x - 0.2383
Degree	Moment (Nm)	Moment (Nm)	Moment (Nm)	Moment (Nm)
-0.1	0.63	-0.53	4.75	-0.97
-0.2	0.37	-0.97	3.68	-1.70
-0.3	0.11	-1.40	2.68	-2.41
-0.4	-0.16	-1.83	1.76	-3.12
-0.5	-0.44	-2.26	0.91	-3.81
-0.6	-0.72	-2.68	0.12	-4.49
-0.7	-1.00	-3.11	-0.62	-5.17
-0.8	-1.29	-3.53	-1.30	-5.83
-0.9	-1.58	-3.95	-1.94	-6.49
-1	-1.88	-4.36	-2.53	-7.13
-1.1	-2.19	-4.78	-3.09	-7.76
-1.2	-2.49	-5.19	-3.62	-8.39
-1.3	-2.81	-5.60	-4.13	-9.00
-1.4	-3.12	-6.00	-4.62	-9.60
-1.5	-3.45	-6.41	-5.09	-10.19
-1.6	-3.77	-6.81	-5.55	-10.78
-1.7	-4.10	-7.21	-6.01	-11.35
-1.8	-4.44	-7.61	-6.47	-11.91
-1.9	-4.78	-8.00	-6.94	-12.46
-2	-5.13	-8.39	-7.42	-13.01
-2.1	-5.48	-8.78	-7.92	-13.54
-2.2	-5.83	-9.17	-8.45	-14.06
-2.3	-6.19	-9.56	-9.00	-14.57
-2.4	-6.56	-9.94	-9.58	-15.07
-2.5	-6.92	-10.32	-10.21	-15.57
-2.6	-7.30	-10.70	-10.88	-16.05
-2.7	-7.68	-11.08	-11.60	-16.52
-2.8	-8.06	-11.45	-12.37	-16.98
-2.9	-8.45	-11.82	-13.21	-17.43
-3	-8.84	-12.19	-14.11	-17.87
-3.1	-9.24	-12.56	-15.08	-18.30
-3.2	-9.64	-12.92	-16.13	-18.72
-3.3	-10.04	-13.28	-17.26	-19.13
-3.4	-10.46	-13.64	-18.48	-19.53

-3.5	-10.87	-14.00	-19.80	-19.92
-3.6	-11.29	-14.36	-21.21	-20.30

Table 4 stiffness of the 4.6mm AFO as measured by both devices.

Path:	**Unloading in the custom-made**	**Loading in the custom-made**	**Unloading in the Instron**	**Loading in the Instron**
Equation:	**y= -0.235x2 + 2.538x + 0.8898**	**y=0.1178x2 + 4.3852x - 0.0954**	**y = 0.8909x3 + 4.4481x2 + 11.999x + 5.9082**	**y = 0.5064x2 + 7.3968x - 0.2383**
Degree	**Stiffness (Nm/Degree)**	**Stiffness (Nm/Degree)**	**Stiffness (Nm/Degree)**	**Stiffness (Nm/Degree)**
-0.1	-6.337	5.327	-47.519	9.729
-0.2	-1.864	4.839	-18.396	8.487
-0.3	-0.358[8]	4.668	-8.949	8.039
-0.4	0.408	4.577	-4.408	7.790
-0.5	0.876	4.517	-1.819	7.620
-0.6	1.196	4.474	-0.196	7.490
-0.7	1.431	4.439	0.882	7.383
-0.8	1.614	4.410	1.625	7.290
-0.9	1.761	4.385	2.153	7.206
-1	1.883	4.363	2.534	7.129
-1.1	1.988	4.342	2.813	7.056
-1.2	2.079	4.323	3.021	6.988
-1.3	2.159	4.305	3.177	6.922
-1.4	2.231	4.288	3.298	6.858
-1.5	2.297	4.272	3.393	6.796
-1.6	2.358	4.256	3.470	6.735
-1.7	2.414	4.241	3.537	6.676
-1.8	2.467	4.226	3.597	6.618
-1.9	2.516	4.212	3.654	6.560
-2	2.563	4.197	3.712	6.503
-2.1	2.608	4.183	3.773	6.447
-2.2	2.651	4.169	3.840	6.391
-2.3	2.692	4.156	3.912	6.336
-2.4	2.731	4.142	3.993	6.281
-2.5	2.770	4.129	4.084	6.226
-2.6	2.807	4.116	4.184	6.172
-2.7	2.843	4.102	4.296	6.118
-2.8	2.878	4.089	4.419	6.064
-2.9	2.913	4.076	4.555	6.010

[8] Values in dark gray fond were considered as outliers.

-3	2.946	4.064	4.703	5.957
-3.1	2.979	4.051	4.866	5.904
-3.2	3.012	4.038	5.042	5.851
-3.3	3.044	4.025	5.232	5.798
-3.4	3.075	4.013	5.437	5.745
-3.5	3.106	4.000	5.656	5.692
-3.6	3.137	3.988	5.891	5.640
Mean stiffness	***2.376***	***4.277***	***3.282***	***6.736***

The differences in stiffness between the measurements (with the Instron E10000 and the custom-made device), for both paths, was calculated in an excel spreadsheet. The mean value for the unloading path was found equal to 0.906 Nm/degree with a standard deviation of 1.47 Nm/degree, whereas the mean value for the loading path was equal to 2.458 Nm/degree with a standard deviation of 0.603 Nm/degree. Once again, the observed difference between the two methods is considerable and it seems that the selection of the technique can greatly alter the results obtained. It is believed that the cause of this variation is that the custom-made method is sensitive to creep and thus the AFO seems to be more flexible when measured there. The author of this thesis professes that the stiffness results from two studies that differ extensively in their philosophy (loading pattern, use of an effigy leg) should not be compared. The most appropriate method for determining the stiffness of an ankle foot orthosis should be assessed by its accuracy and repeatability. The device designed by Bregman et al. (2009) is in favour of this viewpoint and is accompanied by a reliability study. Despite that, as long as the study is followed by the patient's gait analysis, every method can offer the biomechanical ground for the interpretation of the results and the clinical assessment of an AFO.

6 Conclusions and recommendations

6.1 Conclusions

In this study, the implication of using an effigy leg during the testing procedure was investigated. The stiffness testing of the 4.6mm co-polymer AFO showed that the difference in stiffness when a leg is introduced in an AFO is considered noteworthy (μ=5.182 Nm/degree, σ=2.21 Nm/degree for the loading path and μ=2.13 Nm/degree, σ= 1.01 Nm/degree for the unloading path) and It is suggested that an effigy leg should be included in the design of a bench test since it enables the experimenter to mimic the loading of the AFO during normal ambulation.

Furthermore, the mathematical data processing of the Instron testing existing in the literature (Major et al., 2004) was found imprecise. An error equal to 0.8814 Nm/degree with a standard deviation of 0.42595 Nm/degree was found when the distance between the lower jig and the medial malleolus prominence of the 4.6mm co-polymer AFO and the distance connecting the medial malleolus and the upper jig were considered as constants.

Finally, two different methods for determining the stiffness of an ankle foot orthosis were examined in order to confirm whether the selection of the testing apparatus can *significantly* alter the results obtained. The testing of the 4.6 co-polymer AFO revealed that the differences in stiffness between the two measurement methods was found equal to 0.906 Nm/degree with a standard deviation of 1.47 Nm/degree for the unloading path, whereas the mean value for the loading path was equal to 2.458 Nm/degree with a standard deviation of 0.603 Nm/degree. The difference between the two methods is considerable and it is believed that the cause of this variation is that the manual methods are more sensitive to creep and thus the AFO seems to be more flexible when measured there.

6.2 Recommendations

As suggested, an effigy leg should be included in a bench test since it enables the experimenter to mimic the loading of the AFO during normal ambulation while it prevents the orthosis to excessively rotate and bend in other planes than the one loaded. Nevertheless, different designs (material, joints, and prosthetic feet) of a surrogate leg should be tested and the results must be compared with the ones obtained from a functional test. That way, an effigy that can replicate the biomechanical properties of the human limb can be constructed.

In this study, a tape measure was used to determine the deformation of the calf and the sole of the AFO during a compression test. A camera system (such as the Bluehill software) should be used in order to measure those distances more accurately. During this study, the camera of the Instron 10000 was unavailable.

Nowadays, a vast variety of AFO designs is prescribed to stroke patients. Since it is time consuming and cost-inefficient to determine the mechanical properties of an ankle foot orthosis by means of bench testing, more emphasis should be given in developing and validating a finite element analysis model.

7 Bibliography

Bregman, D., De Groot, V., Van Diggele, P., Meulman, H., Houdijk, H. and Harlaar, J. (2010). Polypropylene ankle foot orthoses to overcome drop-foot gait in central neurological patients: A mechanical and functional evaluation. *Prosthetics and orthotics international*, 34(3), pp.293--304.

Bregman, D., Rozumalski, A., Koops, D., De Groot, V., Schwartz, M. and Harlaar, J. (2009). A new method for evaluating ankle foot orthosis characteristics: BRUCE. *Gait & posture*, 30(2), pp.144--149.

Cappa, P., Patane, F. and Pierro, M. (2003). A novel device to evaluate the stiffness of ankle-foot orthosis devices. *Journal of biomechanical engineering*, 125(6), pp.913--917.

Chen, C., Hong, W., Wang, C., Chen, C., Wu, K., Kang, C. and Tang, S. (2010). Kinematic features of rear-foot motion using anterior and posterior ankle-foot orthoses in stroke patients with hemiplegic gait.*Archives of physical medicine and rehabilitation*, 91(12), pp.1862--1868.

CHOWANIEC, Z. (1983). *Effects of polypropylene ankle foot orthoses on hemiplegic gait.*. Ph.D. University of Strathclyde.

Chu, T. and Feng, R. (1998). Determination of stress distribution in various ankle-foot orthoses: Experimental stress analysis. *JPO: Journal of Prosthetics and Orthotics*, 10(1), pp.11--16.

Chu, T., Reddy, N. and Padovan, J. (1995). Three-dimensional finite element stress analysis of the polypropylene, ankle-foot orthosis: static analysis. *Medical engineering \& physics*, 17(5), pp.372--379.

College, S. and Ankle, F. (2014). *Biology 2320 > Sawitzke > Flashcards > Foot and Ankle | StudyBlue*. [online] StudyBlue. Available at: http://www.studyblue.com/notes/note/n/foot-and-ankle/deck/5773985 [Accessed 30 Jul. 2014].

Commons.wikimedia.org, (2014). *File:Cardan-joint intermediate-shaft 3D.png - Wikimedia Commons*. [online] Available at: http://commons.wikimedia.org/wiki/File:Cardan-joint_intermediate-shaft_3D.png [Accessed 2 Aug. 2014].

Deltaorthotics.com, (2014). *Delta Orthotics | Basic Anatomy of the Foot*. [online] Available at: http://deltaorthotics.com/basic-anatomy-of-the-foot/ [Accessed 30 Jul. 2014].

Faraj, A. (2006). Poliomyelitis: orthopaedic management. *Current Orthopaedics*, 20(1), pp.41--46.

Fatone, S., Gard, S. and Malas, B. (2009). Effect of ankle-foot orthosis alignment and foot-plate length on the gait of adults with poststroke hemiplegia. *Archives of physical medicine and rehabilitation*, 90(5), pp.810--818.

Gök H1, Küçükdeveci A, Altinkaynak H, Yavuzer G, Ergin S. (2003). Effects of ankle-foot orthoses on hemiparetic gait. Clinical rehabilitation, 17(2), pp.137--139.

Gail, R. and Taylor, R. (2009). The effect of bilateral AFO use in diplegic cerebral palsy. *Gait & Posture*, Volume 30(Supplement 2), pp.Pages S37–S38.

Hagenbeek, J. (2013). *The direct effects of variations in AFO stiffness on the kinematics* and *kinetics of gait*. Thesis [M. Sc]. University of Strathclyde. Dept. of Biomedical Engineering.

Insolepro.co.uk, (2014). *insole PRO® - THE INSOLE PROFESSIONALS*. [online] Available at: http://www.insolepro.co.uk/biomechanics.html [Accessed 30 Jul. 2014].

Katdare, K. (1999). *The non-linear stiffness of ankle-foot orthoses.* [Thesis PhD]. The biomedical Engineering Graduate Program. University of Minnesota.

Klasson, B., Convery, P. and Raschke, S. (1998). Test apparatus for the measurement of the flexibility of ankle-foot orthoses in planes other than the loaded plane. *Prosthetics and orthotics international*, 22(1), pp.45--53.

Kobayashi, T., Akazawa, Y., Naito, H., Tanaka, M., Hutchins, S. and others, (2010). Design of an automated device to measure sagittal plane stiffness of an articulated ankle-foot orthosis. *Prosthetics and orthotics international*, 34(4), pp.439--448.

Kobayashi, T., Leung, A., Akazawa, Y. and Hutchins, S. (2011). Design of a stiffness-adjustable ankle-foot orthosis and its effect on ankle joint kinematics in patients with stroke. *Gait & posture*, 33(4), pp.721--723.

Kobayashi, T., Leung, A. and Hutchins, S. (2014). Techniques to measure rigidity of ankle-foot orthosis: a review. *Journal of rehabilitation research & development*, 48(5), pp.565-576.

Korthotics.com.au, (2014). *Korthotics - Custom Made*. [online] Available at: http://www.korthotics.com.au/custom-made/afo [Accessed 1 Aug. 2014].

Kubota, K. (2013). *The Rancho ROADMAP: A Tool for AFO and KAFO Prescription - Physical Therapy Products*. [online] Physical Therapy Products. Available at: http://www.ptproductsonline.com/2013/10/the-rancho-roadmap-a-tool-for-afo-and-kafo-prescription/ [Accessed 2 Jul. 2014].

Lin, V. and Bono, C. (2010). *Spinal cord medicine*. [Book]. 1st ed. New York: Demos Medical.

Lunsford, T., Ramm, T. and Miller, J. (1994). Viscoelastic properties of plastic pediatric AFOs. *JPO: Journal of Prosthetics and Orthotics*, 6(1), pp.3--9.

Major, R., Hewart, P. and MacDonald, A. (2004). A new structural concept in moulded fixed ankle foot orthoses and comparison of the bending stiffness of four constructions. *Prosthetics and orthotics international*, 28(1), pp.44--48.

Neviani, R., Borghi, C. and Costi, S. (2012). Effectiveness of AFO orthoses in children affected by cerebral palsy: Clinical evaluation does not always define patient satisfaction. *Gait & Posture*, Volume 35(Supplement 1), pp.Pages S37–S38.

Novacheck, T., Beattie, C., Rozumalski, A., Gent, G. and Kroll, G. (2007). Quantifying the spring-like properties of ankle-foot orthoses (AFOs). *JPO: Journal of Prosthetics and Orthotics*, 19(4), pp.98--103.

Papi, E. (2012). *An investigation of the methodologies for biomechanical assessment of stroke rehabilitation*. Thesis [Ph. D]. University of Strathclyde, Department of Bioengineering.

Petersen, S., Mockford, C. and Rayner, M. (1999). *Coronary heart disease statistics*. 1st ed. London: British Heart Foundation.

Ploeger, H., Bus, S., Brehm, M. and Nollet, F. (2014). Ankle-foot orthoses that restrict dorsiflexion improve walking in polio survivors with calf muscle weakness. *Gait & posture*.

Professionals.ottobockus.com, (2014). *Ottobock - Single-Axis Feet*. [online] Available at:http://professionals.ottobockus.com/cps/rde/xchg/ob_us_en/hs.xsl/1788.html [Accessed 11 Aug. 2014].

Rehabmart.com, (2014). *Afo*. [online] Available at: http://www.rehabmart.com/category/AFO.htm [Accessed 1 Aug. 2014].

Ringleb, S., Armstrong, T., Berglund, L., Kitaoka, H. and Kaufman, K. (2009). Stiffness of the Arizona ankle-foot orthosis before and after modification for gait analysis. *JPO: Journal of Prosthetics and Orthotics*, 21(4), pp.204--207.

Robertson Training Systems, (2011). *Improving Plantar Fasciitis - Robertson Training Systems*. [online] Available at: http://robertsontrainingsystems.com/blog/improving-plantar-fasciitis/ [Accessed 30 Jul. 2014].

Romkes, J. and Brunner, R. (2002). Comparison of a dynamic and a hinged ankle--foot orthosis by gait analysis in patients with hemiplegic cerebral palsy. *Gait & posture*, 15(1), pp.18--24.

Rose, G., Taylor, R., Ferguson, R. and Robb, J. (2009). The effect of bilateral AFO use in diplegic cerebral palsy. *Gait & Posture*, 30(Supplement 2), pp.S37–S38.

Ross, R., Greig, R. and Convery, P. (1999). Comparison of bending stiffness of six different colours of copolymer polypropylene. *Prosthetics and orthotics international*, 23(1), pp.63--71.

Rubin, G. and Dixon, M. (1973). The modern ankle-foot orthoses (AFOs). *Bull Prosthet Res*, 10(19), pp.20--41.

Simpson, J. and Weiner, E. (1989). *The Oxford English dictionary*. 1st ed. Oxford: Clarendon Press.

Singerman, R., Hoy, D. and Mansour, J. (1999). Design changes in ankle-foot orthosis intended to alter stiffness also alter orthosis kinematics. *JPO: Journal of Prosthetics and Orthotics*, 11(3), pp.48--55.

Sumiya, T., Suzuki, Y. and Kasahara, T. (1996a). Stiffness control in posterior-type plastic ankle-foot orthoses: Effect of ankle trimline Part 1: A device for measuring ankle moment. *Prosthetics and orthotics international*, 20(2), pp.129--131.

Sumiya, T., Suzuki, Y. and Kasahara, T. (1996b). Stiffness control in posterior-type plastic ankle-foot orthoses: effect of ankle trimline Part 2: orthosis

characteristics and orthosis/patient matching. *Prosthetics and orthotics international*, 20(2), pp.132--137.

Syngellakis, S., Arnold, M. and Rassoulian, H. (2000). Assessment of the non-linear behaviour of plastic ankle foot orthoses by the finite element method. *Proceedings of the Institution of Mechanical Engineers, Part H: Journal of Engineering in Medicine*, 214(5), pp.527--539.

The International Committee of the Red Cross (ICRC), (2006). *Ankle-foot orthosis, physical rehabilitation programme*. Manufacturing Guidelines. Manufacturing Guidelines.

Trulife.com, (2014). *Matrix Spiral*. [online] Available at: http://trulife.com/all-products/orthotics/matrix-spiral [Accessed 2 Aug. 2014].

Tyson, S. (2013). Archives of Physical Medicine and Rehabilitation. *Physical and Rehabilitation Medicine*, Volume 94(Issue 7), pp.Pages 1377–1385.

Ufrgs.br, (2014). *Homo sapiens diseases - Skeletal apparatus*. [online] Available at: http://www.ufrgs.br/imunovet/molecular_immunology/pathohomotissueskeletal.html [Accessed 1 Aug. 2014].

Uning, R., Osman, A. and Rahim, A. (2008). 3D Finite Element Analysis of Ankle-Foot Orthosis on Patients with Unilateral Foot Drop: A Preliminary Study. *4th Kuala Lumpur International Conference on Biomedical Engineering 2008, IFMBE Proceedings*, 21, pp.pp 366-369.

Usa.autodesk.com, (2014). *Finite Element Analysis - FEA and Simulation Software - Autodesk*. [online] Available at:

http://usa.autodesk.com/adsk/servlet/item?siteID=123112&id=17670721 [Accessed 29 Jun. 2014].

Whiteside, S., Allen, M., Barringer, W., Beiswenger, W. and Brncick, M. (2007). *Practice analysis of certified practitioners in the disciplines of orthotics and prosthetics*. 1st ed. Alexandria, Virginia: American Board for Certification in Orthotics and Prosthetics, Inc.

Winter, D. (1990). *Biomechanics and motor control of human movement*. 1st ed. New York: Wiley.

Xu, G., Zhang, Y. and Lan, Q. (2014). Effect of AFO on gait stability and balance control in patients with hemiparetic stroke. *Annals of Physical and Rehabilitation Medicine*, 57, pp.e21–e22.

Yamamoto, S., Ebina, M., Iwasaki, M., Kubo, S., Kawai, H. and Hayashi, T. (1993a). Comparative study of mechanical characteristics of plastic AFOs. *JPO: Journal of Prosthetics and Orthotics*, 5(2), p.59.

Yamamoto, S., Kubo, S., Ebina, M., Hayashi, T., Iwasak, M., Kawai, H., Kubota, T. and Miyazaki, S. (1993b). Quantification of the effect of dorsi-/plantarflexibility of ankle-foot orthoses on hemiplegic gait: A preliminary report. *JPO: Journal of Prosthetics and Orthotics*, 5(3), p.42.

ISO 8549-1: 1989 Prosthetics and Orthotics - Vocabulary. General terms for external limb prostheses and orthoses. (2014). 1st ed. Geneva, Switzerland: International Organization for Standardization.

8 Appendix 1: The planes of motion of the human foot and the anatomical terms of motion.

The planes of motion of the human foot and the anatomical terms of motion are presented graphically in the figures below.

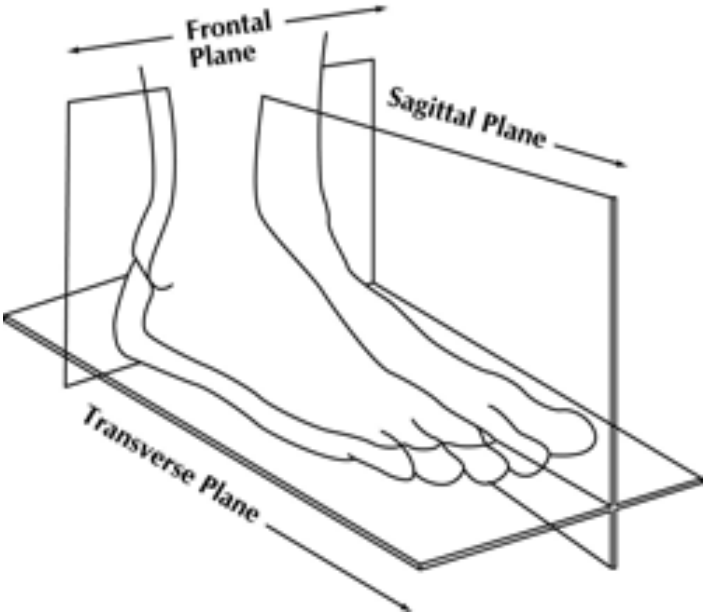

Figure 58 Planes of motion: the human foot (Insolepro.co.uk, 2014)

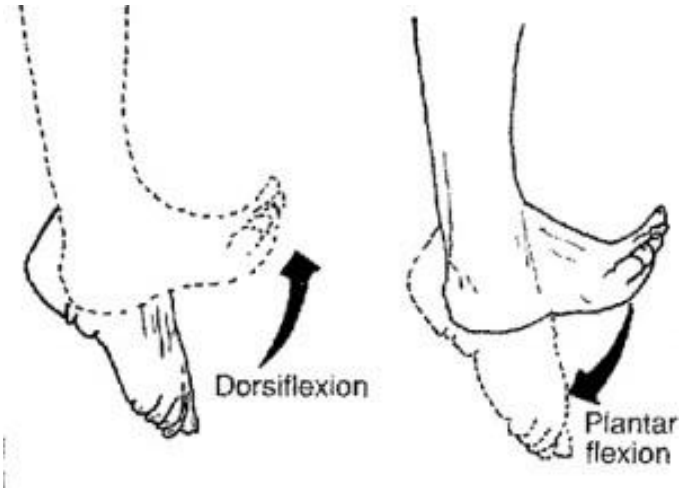

Figure 59 Anatomical terms of motion: dorsiflexion & plantarflexion (Robertson Training Systems, 2011)

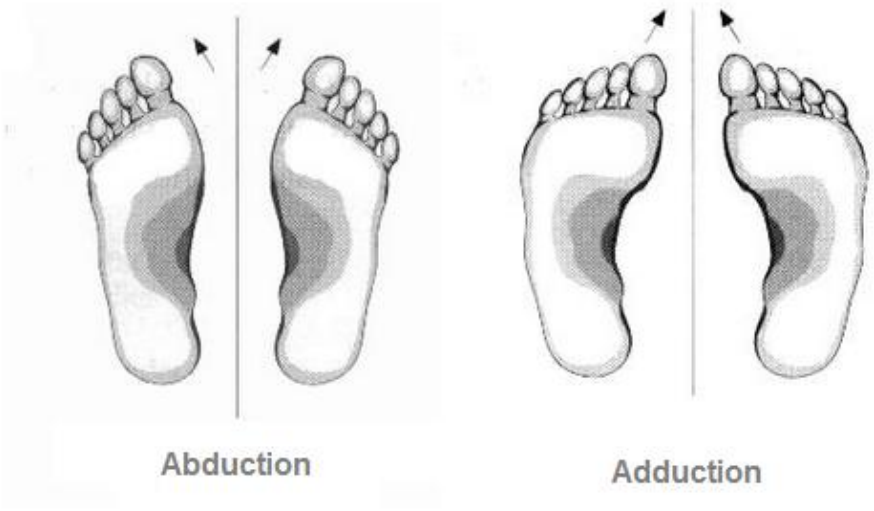

Figure 60 Anatomical terms of motion: abduction & adduction (Deltaorthotics.com, 2014)

Figure 61 Anatomical terms of motion: inversion and eversion (College and Ankle, 2014).